Supplementary information

(±)-Usphenethylones A−C, three pairs of heterodimeric polyketide enantiomers from *Aspergillus ustus* 3.3904

Xiaogang Peng,‡ Shuang Zhou,‡ Junjun Liu, Ying Gao, Jinling Chang, and Hanli Ruan*

School of Pharmacy, Tongji Medical College, Huazhong University of Science and Technology, Hubei Key Laboratory of Natural Medicinal Chemistry and Resource Evaluation, Wuhan 430030, P. R. China

* Correspondence to Hanli Ruan
E-mail: ruanhl@mails.tjmu.edu.cn.

Content

Experimental

General experimental procedures

UV spectra were obtained using a Perkin-Elmer Lambda-25 UV–vis spectrophotometer. A Bruker VERTEX 70 FT-IR microscopic spectroscopy was used for scanning IR spectroscopy with KBr pellets. Optical rotations were measured on a Perkin-Elmer 341 polarimeter. ECD spectra were measured on a JASCO-810 spectrometer. HRESIMS were performed on a Thermo Scientific LC-LTQ-Orbitrap XL spectrometer. NMR spectra were recorded on a Bruker-AM-400 spectrometer with tetramethylsilane (TMS) as the internal standard. Semipreparative HPLC separation were performed on an Agilent 1260 liquid chromatograph with a YMC C_{18} column (250 × 10 mm, 5 μm, Tokyo, Japan). Chiral HPLC analysis and separation were performed on Agilent 1260 and Quiksep-50IID (H&E Co.,Ltd) liquid chromatograph using a CHIRALPAK IG Lot No. T31IG00DE–VF029 (4.6 × 250 mm, 5 μm). Column chromatography (CC) was performed with silica gel (100−200 mesh 200−300 mesh, and 300−400 mesh, Yantai Jiangyou Chemical Inc., Shandong, China), ODS (50 μm, YMC Co. Ltd., Tokyo, Japan), and Sephadex LH-20 (GE Healthcare, Uppsala, Sweden). Thin-layer chromatography (TLC) was performed with silica gel plates (GF-254, Yantai Chemical Industry Research Institute).

Fungal Material

The strain *Aspergillus ustus* 3.3904 used in this work was purchased from China General Microbiological Culture Collection Center (CGMCC). A voucher sample

(RHL20190710) has been preserved in the culture collection center of Tongji Medical College, Huazhong University of Science and Technology.

Fermentation, extraction and isolation

This strain was cultured on PDA medium for 7 days, and then was cut into small pieces to incubate on solid rice medium (250 g rice and 250 mL water for each 1 L Erlenmeyer flask, the total weight of rice was 75 kg) to culture for further 30 days at 25 °C. The fermented rice substrate was extracted five times with EtOAc at room temperature, and the solvent was evaporated under vacuum to afford the EtOAc extract (456 g). The extract (456 g) was subjected to CC on silica gel (petroleum ether/ethyl acetate, step gradient elution 1:0, 10:1, 5:1, 3:1, 2:1, 1:1, 0:1) to obtain six fractions (A−F). Fr. D (15.0 g) was separated by Sephadex LH-20 CC (CH_2Cl_2/MeOH, 1:1) to afford six subfractions (Fr. D1–D6). Fr. D3 (8.0 g) was then separated using an ODS CC with gradient mixtures of MeOH−H_2O (30:70→100:0, v/v) to yield twenty-four subfractions (Fr. D3.1−Fr. D3.24). Fr. D3.14 (468.9 mg) was subjected to CC on silica gel (petroleum ether/ethyl acetate, step gradient elution 1:0, 10:1, 5:1, 2:1, then 1:1) to furnish subfractions D3.14.1−D3.14.10. Fr. D3.14.2 (156.8 mg) was purified by semipreparative HPLC (MeOH/H_2O, 60:40, v = 2.0 mL/min) to afford compound **3** (3.4 mg). Fr. D3.18 (570.4 mg) was subjected to CC on silica gel (petroleum ether/ethyl acetate, step gradient elution 1:0, 10:1, 5:1, 2:1, then 1:1) to furnish subfractions D3.18.1-D3.18.9. Fr. D3.18.1 (120.0mg) was purified by pre-HPLC (MeOH/H_2O, 75:25, v = 2.0 mL/min) to afford compounds **1** (7.0 mg). Fr. D3.18.2 (365.3 mg) was purified by pre-HPLC (MeOH/H_2O, 70:30, v = 2.0 mL/min) to afford compounds **2**

(9.4 mg). Racemic **1**, **2** and **3** were separated by chiral HPLC columns of CHIRALPAK IG Lot No. T31IG00DE–VF029 (4.6 × 250 mm, 5 μm).

*(±)-Usphenethylone A (**1**):* colorless needles; $[\alpha]_D^{25}$ + 9.7 [*c* 0.2, MeOH, (+)-**1**], $[\alpha]_D^{25}$ – 10.0 [*c* 0.2, MeOH, (–)-**1**]; UV (MeOH) λ_{max} (log ε) 205 (4.38), 285 (4.09), 348 (3.26) nm; ECD [MeOH, (+)-**1**] λ_{max} ($\Delta\varepsilon$) 204 (+ 27.17), 226 (– 2.47), 246 (+ 0.72), 277 (– 5.28); ECD [MeOH, (–)-**1**] λ_{max} ($\Delta\varepsilon$) 203 (– 23.56), 222 (+ 3.03), 242 (– 0.43), 276 (+ 4.99); IR (KBr) ν_{max} 3451, 1718, 1695, 1642, 1631, 1586, 1384, 1135, 1064 cm^{-1}; (+)-HRESIMS *m/z* 395.1093 $[M + Na]^+$ (calcd for $C_{20}H_{20}O_7Na$, 395.1107); ^1H and ^{13}C NMR data, see Table 1.

*(±)-Usphenethylone B (**2**):* colorless needles; $[\alpha]_D^{25}$ + 122.1 [*c* 0.2, MeOH, (+)-**2**], $[\alpha]_D^{25}$ – 122.5 [*c* 0.2, MeOH, (–)-**2**]; UV (MeOH) λ_{max} (log ε) 205 (4.33), 286 (4.03), 337 (3.25) nm; ECD [MeOH, (+)-**2**] λ_{max} ($\Delta\varepsilon$) 206 (+ 17.95), 273 (– 3.70), 299 (+ 1.47); ECD [MeOH, (–)-**2**] λ_{max} ($\Delta\varepsilon$) 206 (– 18.80), 276 (+ 3.87), 298 (– 2.13); IR (KBr) ν_{max} 3433, 1712, 1634, 1589, 1124, 1020 cm^{-1}; (+)-HRESIMS *m/z* 425.1191 $[M + Na]^+$ ($C_{21}H_{22}O_8Na$, 425.1212); ^1H and ^{13}C NMR data, see Table 1.

*(±)-Usphenethylone C (**3**):* colorless needles; $[\alpha]_D^{25}$ + 4.3 [*c* 0.2, MeOH, (+)-**3**], $[\alpha]_D^{25}$ – 5.0 [*c* 0.2, MeOH, (–)-**3**]; UV (MeOH) λ_{max} (log ε) 207 (4.76), 228 (4.13), 290 (4.11) nm; ECD [MeOH, (+)-**3**] λ_{max} ($\Delta\varepsilon$) 209 (– 17.26); ECD [MeOH, (–)-**3**] λ_{max} ($\Delta\varepsilon$) 209 (+ 20.52); IR (KBr) ν_{max} 1703, 1579, 1514, 1214, 1126, 1033 cm^{-1}; (+)-HRESIMS *m/z* 383.1462 $[M + Na]^+$ ($C_{20}H_{24}O_6Na$, 383.1471); ^1H and ^{13}C NMR data, see Table 1.

X-ray crystallographic analysis of compounds 1–3

Crystals of compounds **1**–**3** were successfully obtained from CH_2Cl2/MeOH (1:1) at

room temperature. Crystallographic data of **1**, (+)-**1**, (-)-**1**, **2**, (+)-**2**, (-)-**2** (+)-**3**, and (-)-**3** were collected on a Bruker APEX-II CCD diffractometer using monochromatized Cu Kα radiation. Crystallographic data of (+)-**1**, (-)-**1**, (+)-**2**, (-)-**2** (+)-**3**, and (-)-**3** have been deposited in the Cambridge Crystallographic Data Centre (deposition number: CCDC 2104478−2104483, 2124877, and 2124876). Copies of these data can be obtained free of charge via www.ccdc.cam.ac.uk/deposit (or from the CCDC, 12 Union Road, Cambridge CB2 1EZ, UK; fax: +44 1223 336033; deposit@ccdc.cam.ac.uk).

*Crystal data of **1**:* $C_{20}H_{20}O_7$ (M = 372.36 g/mol): monoclinic, space group $P2_1/c$ (no. 14), a = 13.66489(13) Å, b = 15.50084(13) Å, c = 8.21733(8) Å, β = 102.5797(9)°, V = 1698.79(3) Å^3, Z = 4, T = 100.00(10) K, μ(CuKα) = 0.928 mm^{-1}, *Dcal* = 1.456 g/cm^3, 19485 reflections measured (6.628° ≤ 2θ ≤ 147.85°), 3396 unique (R_{int} = 0.0301, R_{sigma} = 0.0184) which were used in all calculations. The final R_1 was 0.0332 (I > 2σ(I)) and wR_2 was 0.0900 (all data).

*Crystal data of (+)-**1**:* $C_{20}H_{22}O_8$ (M = 390.37 g/mol): monoclinic, space group $P2_1$ (no. 4), a = 14.1584(16) Å, b = 4.6034(5) Å, c = 14.9562(16) Å, β = 113.249(5)°, V = 895.64(17) Å^3, Z = 2, T = 100.00(1) K, μ(CuKα) = 0.603 mm^{-1}, *Dcal* = 1.448 g/cm^3, 19710 reflections measured (5.596° ≤ 2θ ≤ 104.858°), 3074 unique (R_{int} = 0.0749, R_{sigma} = 0.0478) which were used in all calculations. The final R_1 was 0.0851 (I > 2σ(I)) and wR_2 was 0.2370 (all data).

*Crystal data of (-)-**1**:* $C_{20}H_{22}O_8$ (M = 390.37 g/mol): monoclinic, space group $P2_1$ (no. 4), a = 14.126(4) Å, b = 4.5761(13) Å, c = 14.955(5) Å, β = 113.280(12)°, V = 888.0(5) Å^3, Z = 2, T = 100.00(2) K, μ(CuKα) = 0.609 mm^{-1}, *Dcal* = 1.460 g/cm^3, 16506

reflections measured (5.596° ≤ 2θ ≤ 109.988°), 3317 unique (R_{int} = 0.0753, R_{sigma} = 0.0569) which were used in all calculations. The final R_1 was 0.0435 (I > 2σ(I)) and wR_2 was 0.1169 (all data).

Crystal data of ***2****:* $C_{21}H_{22}O_8$ (*M* = 402.38 g/mol): monoclinic, space group *P*-1, *a* = 4.53147(10) Å, *b* = 14.6487(2) Å, *c* = 28.5217(4) Å, β = 85.9500(14)°, *V* = 1882.16(6) Å^3, *Z* = 4, *T* = 99.99(10) K, μ(CuKα) = 0.921 mm^{-1}, *Dcal* = 1.420 g/cm^3, 39721 reflections measured (6.054° ≤ 2θ ≤ 148.65°), 7433 unique (R_{int} = 0.0630) which were used in all calculations. The final R_1 was 0.0564 (I > 2σ(I)) and wR_2 was 0.1604 (all data).

*Crystal data of (+)-****2****:* $C_{42}H_{44}O_{16}$ (*M* = 804.77 g/mol): monoclinic, space group $P2_12_12_1$ (no. 19), *a* = 4.5505(2) Å, *b* = 17.1723(8) Å, *c* = 48.042(2) Å, *V* = 3754.2(3) Å^3, *Z* = 4, *T* = 100(2) K, μ(CuKα) = 0.588 mm^{-1}, *Dcal* = 1.424 g/cm^3, 22765 reflections measured (3.2° ≤ 2θ ≤ 92.948°), 4878 unique (R_{int} = 0.1192, R_{sigma}= 0.0631) which were used in all calculations. The final R_1 was 0.0381 (I > 2σ(I)) and wR_2 was 0.0941 (all data).

*Crystal data of (-)-****2****:* $C_{21}H_{22}O_8$ (*M* = 402.38 g/mol): monoclinic, space group $P2_12_12_1$ (no. 19), *a* = 4.5507(10) Å, *b* = 17.161(4) Å, *c* = 48.011(10) Å, *V* = 3749.4(14) Å^3, *Z* = 8, *T* = 100(1) K, μ(CuKα) = 0.589 mm^{-1}, *Dcal* = 1.426 g/cm^3, 53389 reflections measured (3.202° ≤ 2θ ≤ 101.332°), 5725 unique (R_{int} = 0.0865, R_{sigma}= 0.0529) which were used in all calculations. The final R_1 was 0.0461 (I > 2σ(I)) and wR_2 was 0.1113 (all data).

*Crystal data of (+)-****3****:* $C_{20}H_{24}O_6$ (*M* = 360.39 g/mol): orthorhombic, space group $P2_1$

(no. 4), a = 8.5427(4) Å, b = 15.2194(8) Å, c = 14.1219(7) Å, β = 91.418(2)°, V = 1835.49(16) Å^3, Z = 4, T = 100.0 K, μ(CuKα) = 0.505 mm^{-1}, *Dcal* = 1.304 g/cm^3, 43116 reflections measured (5.446° ≤ 2θ ≤ 114.132°), 7371 unique (R_{int} = 0.0400, R_{sigma} = 0.0273) which were used in all calculations. The final R_1 was 0.0351 (I > 2σ(I)) and wR_2 was 0.0970 (all data).

*Crystal data of (-)-**3**:* $C_{20}H_{24}O_6$ (M = 360.39 g/mol): orthorhombic, space group $P2_12_12_1$ (no. 19), a = 8.6051(4) Å, b = 14.1919(6) Å, c = 15.2989(6) Å, V = 1868.34(14) Å^3, Z = 4, T = 200.0 K, μ(CuKα) = 0.496 mm^{-1}, *Dcal* = 1.281 g/cm^3, 32268 reflections measured (10.262° ≤ 2θ ≤ 118.156°), 4055 unique (R_{int} = 0.0539, R_{sigma} = 0.0233) which were used in all calculations. The final R_1 was 0.0292 (I > 2σ(I)) and wR_2 was 0.0793 (all data).

ECD calculation method

The conformations of (+)-**1**, (-)-**1**, (+)-**2**, and (-)-**2** generated by BALLOON were subjected to semiempirical PM3 quantum mechanical geometry optimizations using the Gaussian 09 program. The X-ray single diffraction tridimensional structure of (+)-**1**, (-)-**1**, (+)-**2**, and (-)-**2** were used as geometry input. Duplicate conformations were identified and removed when the root-mean-square (RMS) distance was less than 0.5 Å for any two geometry-optimized conformations. The remaining conformations were further optimized at the B3LYP/6-31G (d) level in MeOH with the IEFPCM solvation model using Gaussian 09, and the duplicate conformations emerging after these calculations were removed according to the same RMS criteria above. The harmonic vibrational frequencies were calculated to confirm the stability of the final conformers.

The electronic circular dichroism (ECD) spectrum were calculated for each conformer using the TDDFT methodology at the B3LYP/6-311+G (d, p)//B3LYP/6-31G (d) level with MeOH as solvent by the IEFPCM solvation model implemented in Gaussian 09 program. The ECD spectra for each conformer were simulated using a Gaussian function with a bandwidth σ of 0.4 eV. The spectra were combined after Boltzmann weighting according to their population contributions and UV correction was applied.

Cytotoxicity assay

The cytotoxicity assay was tested using MTT method. HCT116 human colon carcinoma and HeLa human cervical carcinoma cell lines, were cultured in DMEM medium (Hyclone) supplemented with 10% heat-inactivated fetal bovine serum (Sijiqing, Hangzhou, People's Republic of China), 100 U/mL penicillin, and 100 mg/mL streptomycin and were incubated at 5% CO_2 in a 37 °C incubator (MCO-18AC, Panasonic). 90 μL cells were seeded into each well of a 96-well culture plates (5000 cells/well). After 24 h incubation, cells were pretreated with 50 μM of the test compounds and 2.5 μM of positive drug. After 24 h of treatment, 15 μL of the MTT solution (5 mg/mL) was added into each well followed by 4 h incubation at 37 °C, DMSO (100 μL/well) was added after that the supernatant was removed. The absorbance was measured at 490 nm with a microplate reader (Bio-Tek Synergy 2 reader). Doxorubicin hydrochloride was used as the positive control.

Immunosuppressive activity assay

Male BALB/c mice (8 weeks old) were purchased from Hubei Provincial Center for Disease Control and Prevention and were housed in SPF conditions (12 h light/12 h

dark alternating photoperiod, 22 ± 1 °C, 55% ± 5% relative humidity). All experimental procedures were approved by the Ethical Committee of Huazhong University of Science and Technology (No. SYXK2016-0057).

Male BALB/c mice were sacrificed by cervical dislocation, and were disinfected for 5 minutes by 75% alcohol; the fresh spleens were dissected and moved into an EP tube (1.5 mL) supplemented with heat-inactivated Phosphate Buffered Saline (PBS) under aseptic conditions. The fresh spleens were grinded in a 40-μm filter screen to prepare mononuclear cell suspensions. Then Red Blood Cell Lysis Buffer was used to crack the erythrocytes. Lymphocytes were washed 2 times and suspended in RPMI 1640 medium (Hyclone, Logan, UT) supplemented with 10% FBS (Sijiqing, Hangzhou, People's Republic of China), penicillin (100 U/mL, Hyclone, Logan, UT) and streptomycin (100 μg/mL, Hyclone, Logan, UT).

The 6×10^5 (180 μL per well) spleen cells for in 96 well flat plates were cultured at 5% CO_2-containing and 37 °C in a humidified incubator for 36 h in the presence or absence of compounds (20 μL compounds or PBS). The cultures were stimulated with 5 μg/mL of concanavalin A (ConA, Sigma, USA) or 10 μg/mL of lipopolysaccharide (LPS, Sigma, USA) to induce T cells or B cells proliferative responses, respectively. Cyclosporin A (CsA, Sigma, USA) for T cells and mycophenolate mofetil (MMF, Sigma, USA) for B cells were used as positive controls. Subsequently, 20 μL MTT (5 mg/mL) solution was added to each well and incubated for another 4 h. Then, all 96-well flat plates were centrifuged (3000 rpm, 10 min), and 100 μL DMSO was added to dissolve precipitates after the supernatant was removed. At last, the OD values were

measured with a microplate reader (Bio-Tek Synergy 2) at 490 nm. The average optical density formed in control cells was taken as 0% proliferation inhibition, and the treatments of compounds **1−3** and positive drugs were expressed as a percentage of the control.

Antibacterial assay

The tested bacteria strains *Escherichia coli* ATCC35218, *Staphylococcus aureus* ATCC25923 were purchased from Tongji Hospital of Huazhong University of Science and Technology. *Candida albicans* ATCC10231 was purchased from Shanghai Conservation Biotechnology Center. All these strains were cultured in Mueler-Hinton II broth (MHB) at 37 °C overnight with shaking (200 rpm). Then, 90 μL MHB broth with the appropriate density of 5×10^5 CFU/mL bacteria or fungus were seeded at 96-well culture plates. Various concentrations of the test compounds were then diluted in fresh MHB broth was added to each well. Plates were covered and incubated at 37 °C for 24 h. Inhibition rate were determined using photometry at OD_{600} nm. Streptomycin and amphotericin B were used as positive inhibitor controls.

DPPH radical scavenging activity assay

First, 90 μL of a 1.5×10^{-4} μM EtOH solution of DPPH radical was added in a well of a 96-well plate. Then, 10 μL of diluted samples, standard antioxidant solutions, or EtOH (control) was added to 96-well plate. After 30 min of incubation at room temperature (25 °C). The butyl hydroxyanisole (BHA) and trolox were used as positive controls. The absorbance of the reaction mixture at 517 nm was measured at steady state after 30 min of incubation at room temperature (25 °C) using a microplate reader.

The EC_{50} value was defined as the concentration of sample that scavenges 50% of the DPPH radical, which was estimated using GraphPad Prism 5.

ABTS radical scavenging activity assay

ABTS radical was produced by the reaction between 7.0×10^{-3} μM ABTS and 2.45×10^{-3} μM potassium persulfate in H_2O for 12 h in the dark at room temperature. The ABTS radical solution was diluted approximately 20 times with H_2O. Then, 90 μL of ABTS radical solution was added in a well of a 96-well plate. The reaction was initiated by adding 10 μL of sample solution disolved in DMSO to ABTS radical solution. After 7 min at 25 °C, the absorbance at 734 nm was recorded. The EC_{50} values of the test compounds, which lead to 50% loss of the ABTS radical, were calculated in the same way as described in the DPPH assay. The butyl hydroxyanisole (BHA) and trolox were used as positive controls.

Table S1. Cytotoxicity of **1**−**3** against two cancer cell lines

Compounds	IC_{50} value (μM ± SD)	
	HCT116	HeLa
(+)-**1**	>40	>40
(-)-**1**	>40	>40
(+)-**2**	>40	>40
(-)-**2**	>40	>40
(+)-**3**	>40	>40
(-)-**3**	>40	>40
doxorubicin hydrochloride	0.34 ± 0.07	0.20 ± 0.01

Table S2. Antimicrobial activity of compounds **1**−**3** (MIC in μM)[a]

Compounds	bactera		fungus
	Escherichia coli	*Staphylococcus aureus*	*Candida albicans*
(+)-**1**	>50	>50	>50
(-)-**1**	>50	>50	>50
(+)-**2**	>50	>50	>50
(-)-**2**	>50	>50	>50
(+)-**3**	>50	>50	>50
(-)-**3**	>50	>50	>50
streptomycin	2.15	1.72	NT[b]
amphotericin B	NT	NT	0.05

[a]MIC: minimal inhibitory concentration values. [b]NT: not tested

Table S3. DPPH and ABTS radical scavenging activity of compounds **1**−**3**

Compounds	EC_{50} value (μM ± SD)	
	DDPH	$ABTS^{+}$
(+)-**1**	>100	>100
(-)-**1**	>100	>100
(+)-**2**	>100	>100
(-)-**2**	>100	>100
(+)-**3**	>100	>100
(-)-**3**	>100	>100
BHA	67.13 ± 1.85	57.97 ±0.87
Trolox	51.76 ± 1.85	58.79 ± 0.02

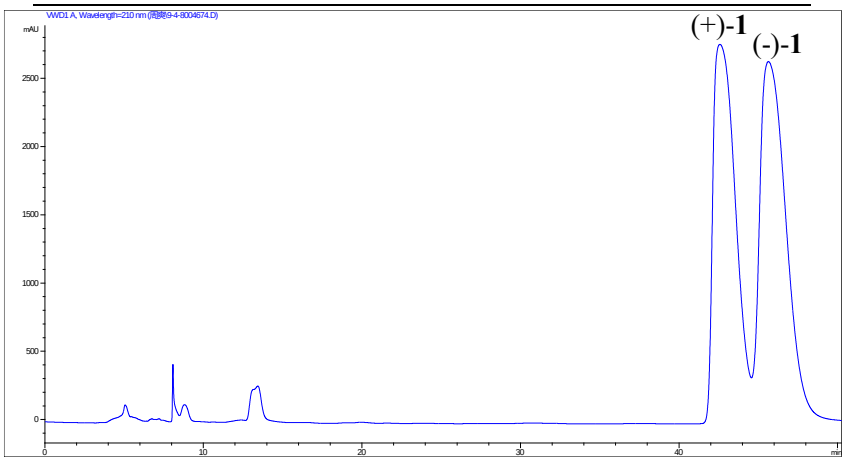

Figure S1. Chiral analysis and preparation of (±)-**1** (CHIRALPAK IG Lot No. T31IG00DE–VF029, 5 μm, 4.6 mm × 250 mm; Acetonitrile/Water = 75:25; flowing speed: 0.4 mL/min; 210 nm of UV detection wavelength).

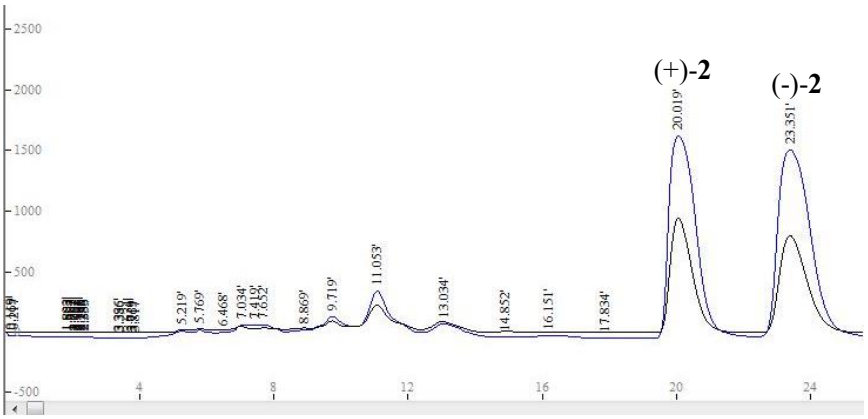

Figure S2. Chiral analysis and preparation of (±)-**2** (CHIRALPAK IG Lot No. T31IG00DE–VF029, 5 μm, 4.6 mm × 250 mm; Acetonitrile/Water = 80:20; flowing speed: 0.4 mL/min; blue line for 210 nm and black line for 254 nm of UV detection wavelength).

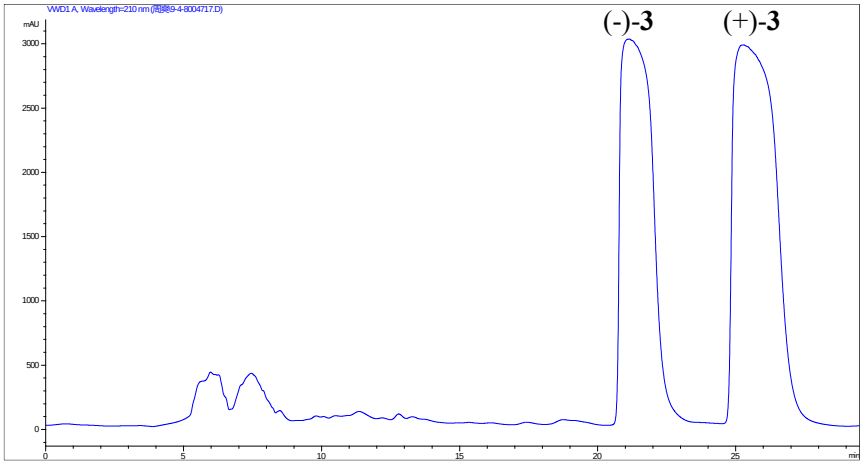

Figure S3. Chiral analysis and preparation of (±)-**3** (CHIRALPAK IG Lot No. T31IG00DE–VF029, 5 μm, 4.6 mm × 250 mm; Acetonitrile/Water = 80:20; flowing speed: 0.4 mL/min; 210 nm of UV detection wavelength).

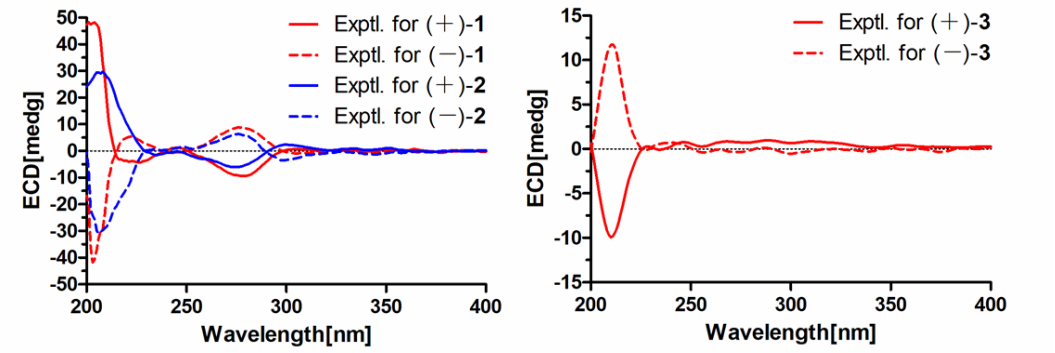

Figure S4. Experimental ECD spectra of **1**−**3**.

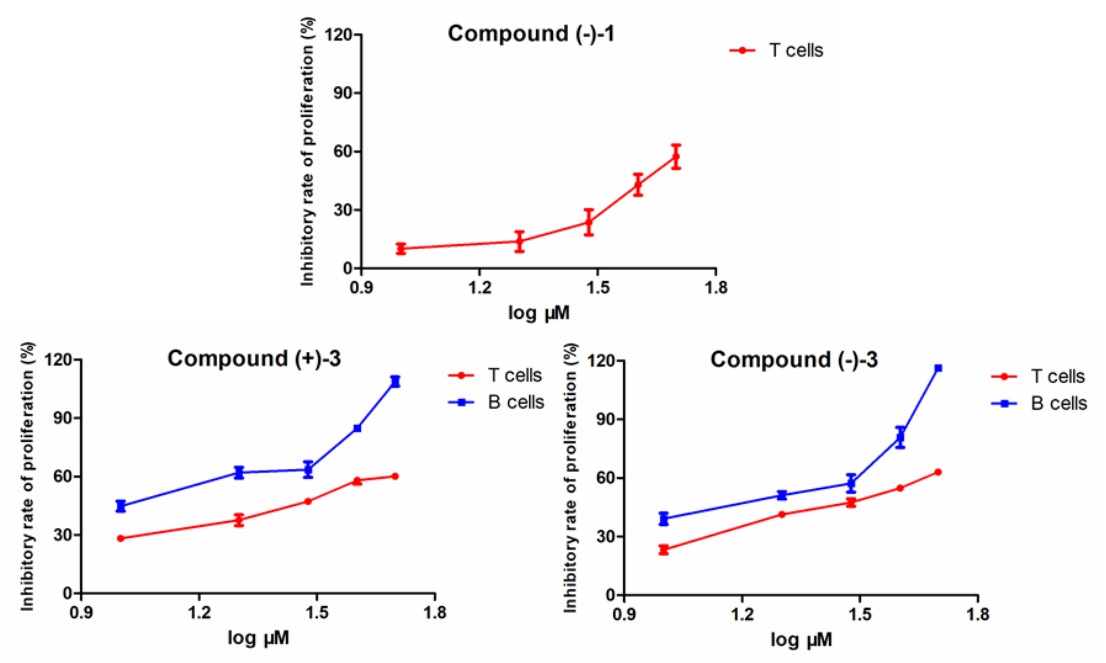

Figure S5. The concentration-response curves of immunosuppressive effects of compounds (-)-**1** and (±)-**3** on murine lymphocyte proliferation induced by ConA (5 μg/mL) or LPS (10 μg/mL).

Computational ECD data of 1 and 2

Table S4. Important thermodynamic parameters (a.u.) and Boltzmann distribution of the optimized compound (+)-**1** at B3LYP/6-311+G(d,p)//B3LYP/6-31G(d) level in methanol

Conformation	Internal Energy	%
1	-1300.718745	82.44%
2	-1300.717289	17.56%

Table S5. Important thermodynamic parameters (a.u.) and Boltzmann distribution of the optimized compound (-)-**1** at B3LYP/6-311+G(d,p)//B3LYP/6-31G(d) level in methanol

Conformation	Internal Energy	%
1	-1300.718745	100.00%

Table S6. Important thermodynamic parameters (a.u.) and Boltzmann distribution of the optimized compound (+)-**2** at B3LYP/6-311+G(d,p)//B3LYP/6-31G(d) level in methanol

Conformation	Internal Energy	%
1	-1415.24605	99.88%

Table S7. Important thermodynamic parameters (a.u.) and Boltzmann distribution of the optimized compound (-)-**2** at B3LYP/6-311+G(d,p)//B3LYP/6-31G(d) level in methanol

Conformation	**Internal Energy**	**%**
1	-1415.246048	99.87%

Table S8. Optimized coordinates of compound (+)-**1** at B3LYP/6-31G(d) level in methanol

Conformation 1							
Atom	**X**	**Y**	**Z**	**Atom**	**X**	**Y**	**Z**
C	2.509	1.188	0.653	O	-0.085	-2.015	-0.242
C	4.416	-0.07	-0.204	O	4.027	-2.332	-0.931
C	1.681	0.077	0.413	O	4.738	2.138	0.538
C	2.187	-1.107	-0.129	H	2.075	2.083	1.08
C	3.864	1.123	0.346	H	6.443	0.715	-0.339
C	3.556	-1.178	-0.427	H	1.444	-2.719	-1.366
C	-2.053	0.673	-0.237	H	1.57	-3.119	0.351
C	-3.966	-0.587	0.695	H	-0.246	0.478	-1.383
C	-2.553	-0.37	0.496	H	-0.343	1.946	-0.422
C	-4.804	0.31	0.105	H	0.054	0.728	1.654
C	-2.966	1.588	-0.859	H	0.067	-1.726	1.8
C	5.822	-0.172	-0.53	H	-4.028	-1.709	2.537
C	1.307	-2.318	-0.358	H	-4.029	-2.704	1.085
C	-0.574	0.877	-0.414	H	-5.5	-1.848	1.564
C	0.199	0.17	0.72	H	-6.561	0.56	-2.04
C	-0.354	-1.243	0.909	H	-8.008	-0.012	-1.19
C	-4.413	-1.772	1.513	H	-6.654	-1.121	-1.48
C	-6.917	-0.087	-1.233	H	5.129	4.022	1.145
C	4.259	3.368	1.09	H	3.849	3.214	2.094
C	-6.305	0.331	0.118	H	3.498	3.818	0.443
O	-2.681	2.553	-1.553	H	-6.682	-0.314	0.914
O	6.352	-1.191	-1.005	H	-6.623	1.353	0.359
O	-1.759	-1.283	1.116	H	5.004	-2.2	-1.087
O	-4.322	1.349	-0.638				
Conformation 2							
Atom	**X**	**Y**	**Z**	**Atom**	**X**	**Y**	**Z**
C	-1.846	1.167	-0.85	O	-0.553	-2.772	-1.797
C	-3.402	0.277	0.807	O	-3.381	-2.1	1.183
C	-1.363	-0.132	-1.095	O	-3.377	2.588	0.383
C	-1.895	-1.233	-0.42	H	-1.436	2.003	-1.399
C	-2.853	1.376	0.086	H	-4.793	1.488	1.965

C	-2.902	-1.023	0.535	H	-0.91	-3.037	0.229
C	1.788	0.53	-1.085	H	-2.265	-3.308	-0.869
C	2.808	-0.84	0.704	H	0.424	1.701	-2.24
C	1.918	-0.664	-0.419	H	1.349	0.569	-3.192
C	3.531	0.25	1.081	H	-0.786	-0.427	-3.126
C	2.577	1.651	-0.67	H	0.989	-2.01	-2.8
C	-4.444	0.46	1.793	H	3.163	-2.963	0.635
C	-1.42	-2.645	-0.661	H	1.911	-2.484	1.776
C	0.827	0.685	-2.232	H	3.616	-2.216	2.172
C	-0.288	-0.374	-2.149	H	6.264	-0.46	1.124
C	0.364	-1.744	-1.942	H	6.681	0.571	2.506
C	2.884	-2.194	1.364	H	6.11	1.303	0.994
C	5.987	0.449	1.668	H	-3.435	4.587	0.116
C	-2.874	3.745	-0.29	H	-3.043	3.677	-1.37
C	4.54	0.362	2.188	H	-1.806	3.883	-0.089
O	2.585	2.769	-1.165	H	4.306	1.267	2.762
O	-4.953	-0.47	2.444	H	4.44	-0.482	2.873
O	1.221	-1.769	-0.764	H	-4.083	-1.768	1.81
O	3.419	1.44	0.422				

Table S9. Optimized coordinates of compound (-)-**1** at B3LYP/6-31G(d) level in methanol

Conformation 1							
Atom	**X**	**Y**	**Z**	**Atom**	**X**	**Y**	**Z**
C	2.509	1.188	-0.653	O	-0.085	-2.015	0.242
C	4.416	-0.07	0.204	O	4.027	-2.332	0.931
C	1.681	0.077	-0.413	O	4.738	2.138	-0.538
C	2.187	-1.107	0.129	H	2.075	2.083	-1.08
C	3.864	1.123	-0.346	H	6.443	0.715	0.339
C	3.556	-1.178	0.427	H	1.57	-3.119	-0.351
C	-2.053	0.673	0.237	H	1.444	-2.719	1.366
C	-3.966	-0.587	-0.695	H	-0.246	0.478	1.383
C	-2.553	-0.37	-0.496	H	-0.343	1.946	0.422
C	-4.804	0.31	-0.105	H	0.054	0.728	-1.653
C	-2.966	1.588	0.859	H	0.067	-1.726	-1.8
C	5.822	-0.172	0.53	H	-4.028	-1.709	-2.537
C	1.307	-2.318	0.358	H	-5.5	-1.848	-1.564
C	-0.574	0.877	0.414	H	-4.029	-2.704	-1.085
C	0.199	0.17	-0.72	H	-6.654	-1.121	1.48
C	-0.354	-1.243	-0.909	H	-8.009	-0.012	1.19
C	-4.413	-1.772	-1.513	H	-6.561	0.56	2.04
C	-6.917	-0.087	1.233	H	3.499	3.819	-0.444
C	4.259	3.368	-1.09	H	3.849	3.214	-2.094

C	-6.305	0.331	-0.118	H	5.129	4.022	-1.145
O	-2.681	2.553	1.553	H	-6.682	-0.314	-0.914
O	6.352	-1.191	1.005	H	-6.623	1.353	-0.359
O	-1.759	-1.283	-1.116	H	5.004	-2.2	1.087
O	-4.322	1.349	0.638				

Table S10. Optimized coordinates of compound (+)-**2** at B3LYP/6-31G(d) level in methanol

Conformation 1							
Atom	**X**	**Y**	**Z**	**Atom**	**X**	**Y**	**Z**
C	-2.253	-1.573	0.716	O	-4.116	1.727	-0.973
C	-4.283	-0.517	-0.134	O	-4.394	-2.711	0.7
C	-1.532	-0.406	0.417	O	-1.778	2.966	0.486
C	-2.155	0.715	-0.138	H	-1.733	-2.415	1.155
C	-3.617	-1.634	0.447	H	-6.231	-1.489	-0.191
C	-3.532	0.656	-0.417	H	0.308	-0.768	-1.459
C	2.19	-0.764	-0.423	H	0.576	-2.17	-0.435
C	4.054	0.673	0.334	H	0.196	-0.889	1.598
C	2.653	0.345	0.234	H	-1.582	2.333	-1.464
C	4.919	-0.175	-0.288	H	0.021	1.56	1.646
C	3.13	-1.635	-1.066	H	4.126	1.84	2.145
C	-5.698	-0.56	-0.438	H	3.999	2.802	0.676
C	0.723	-1.087	-0.494	H	5.542	2.047	1.106
C	-0.034	-0.383	0.653	H	6.852	-0.998	1.602
C	-1.387	1.983	-0.444	H	8.188	-1.095	0.438
C	0.426	1.068	0.757	H	6.785	-2.166	0.269
C	4.461	1.905	1.103	H	-4.604	-4.603	1.37
C	7.1	-1.156	0.547	H	-3.367	-3.663	2.252
C	-3.794	-3.88	1.268	H	-3.02	-4.283	0.606
C	-1.358	4.284	0.133	H	-1.743	4.951	0.907
C	6.418	-0.101	-0.345	H	-1.773	4.579	-0.841
O	2.878	-2.652	-1.696	H	-0.266	4.361	0.095
O	-6.325	0.381	-0.954	H	6.72	-0.258	-1.388
O	1.831	1.221	0.871	H	6.755	0.899	-0.064
O	4.473	-1.279	-0.956	H	-5.077	1.492	-1.111
O	0.023	1.77	-0.41				

Table S11. Optimized coordinates of compound (-)-**2** at B3LYP/6-31G(d) level in methanol

Conformation 1							
Atom	**X**	**Y**	**Z**	**Atom**	**X**	**Y**	**Z**
C	2.253	-1.573	0.716	O	4.117	1.727	-0.972
C	4.283	-0.517	-0.134	O	4.393	-2.712	0.7

C	1.532	-0.406	0.417	O	1.778	2.966	0.486
C	2.155	0.715	-0.138	H	1.732	-2.415	1.155
C	3.617	-1.635	0.447	H	6.231	-1.49	-0.191
C	3.532	0.656	-0.417	H	-0.577	-2.169	-0.435
C	-2.19	-0.764	-0.423	H	-0.308	-0.767	-1.459
C	-4.054	0.674	0.334	H	-0.196	-0.888	1.598
C	-2.653	0.346	0.234	H	1.583	2.333	-1.465
C	-4.92	-0.175	-0.287	H	-0.021	1.561	1.646
C	-3.13	-1.635	-1.065	H	-3.998	2.802	0.676
C	5.698	-0.561	-0.438	H	-4.127	1.841	2.144
C	-0.723	-1.087	-0.495	H	-5.541	2.049	1.105
C	0.034	-0.382	0.653	H	-6.785	-2.168	0.265
C	1.387	1.983	-0.444	H	-8.188	-1.096	0.437
C	-0.426	1.068	0.757	H	-6.852	-1.002	1.601
C	-4.461	1.906	1.103	H	4.603	-4.603	1.369
C	-7.1	-1.158	0.546	H	3.019	-4.283	0.606
C	3.793	-3.881	1.267	H	3.366	-3.664	2.252
C	1.359	4.284	0.133	H	1.744	4.951	0.907
C	-6.419	-0.101	-0.344	H	0.266	4.361	0.096
O	-2.878	-2.652	-1.695	H	1.773	4.579	-0.841
O	6.325	0.38	-0.954	H	-6.756	0.898	-0.061
O	-1.831	1.222	0.87	H	-6.721	-0.256	-1.387
O	-4.474	-1.278	-0.955	H	5.077	1.492	-1.111
O	-0.023	1.77	-0.41				

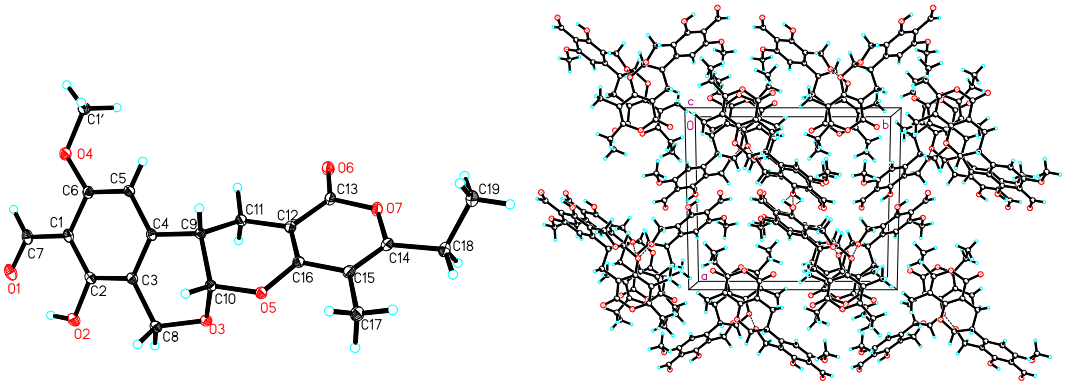

Figure S6. X-ray ORTEP drawing of **1** at the 50% probability levels.

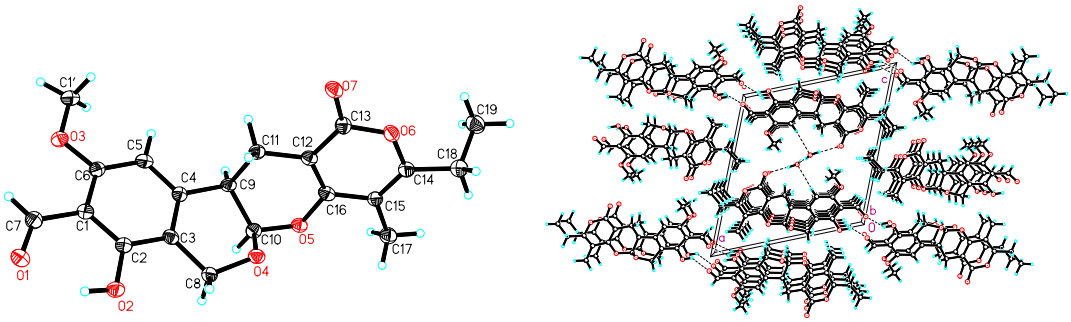

Figure S7. X-ray ORTEP drawing of **(+)-1** at the 50% probability levels.

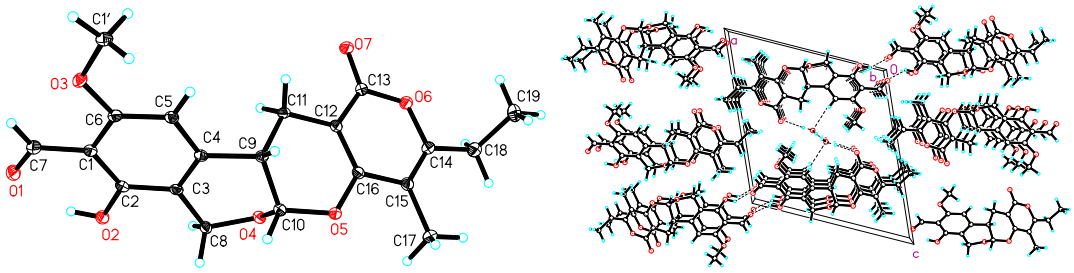

Figure S8. X-ray ORTEP drawing of **(-)-1** at the 50% probability levels.

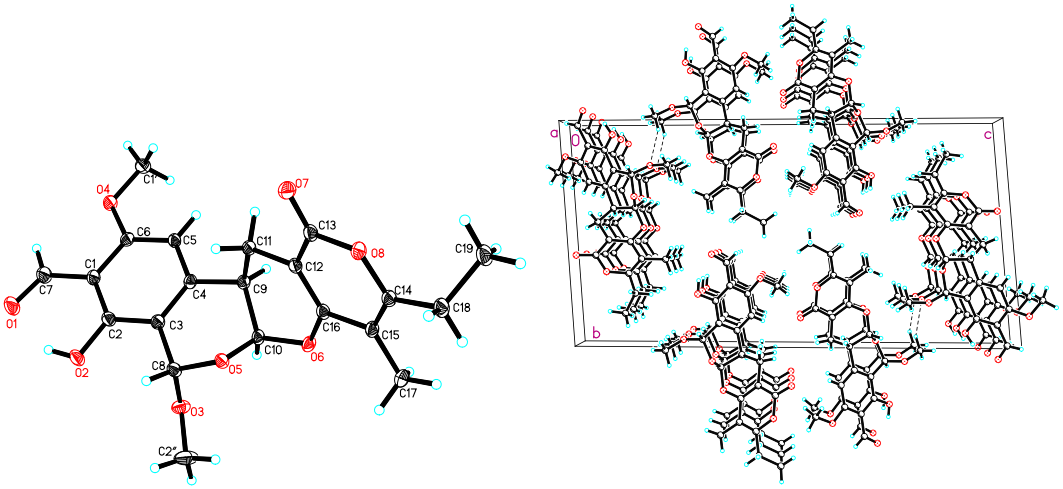

Figure S9. X-ray ORTEP drawing of **2** at the 50% probability levels.

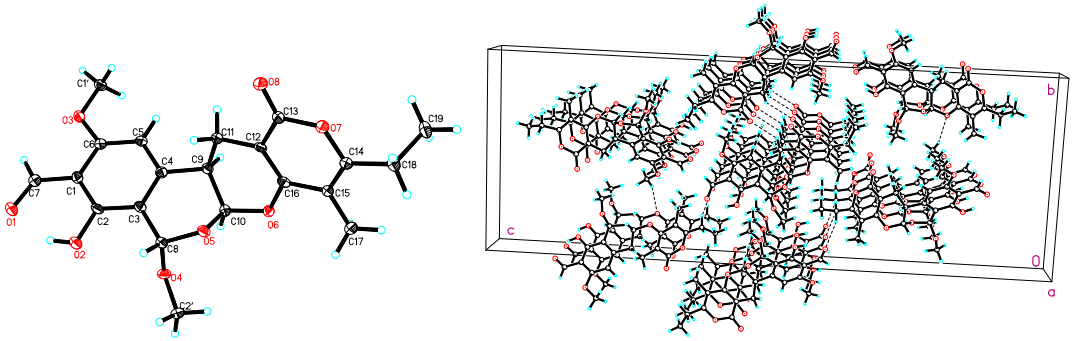

Figure S10. X-ray ORTEP drawing of **(+)-2** at the 50% probability levels.

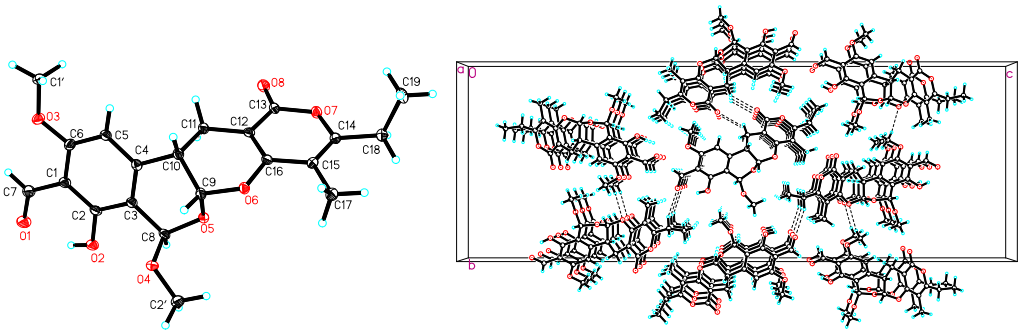

Figure S11. X-ray ORTEP drawing of **(-)-2** at the 50% probability levels.

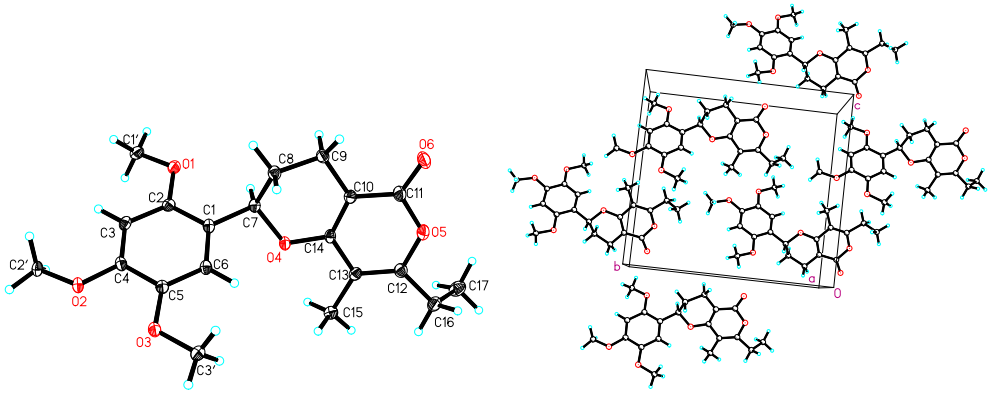

Figure S12. X-ray ORTEP drawing of **(+)-3** at the 50% probability levels.

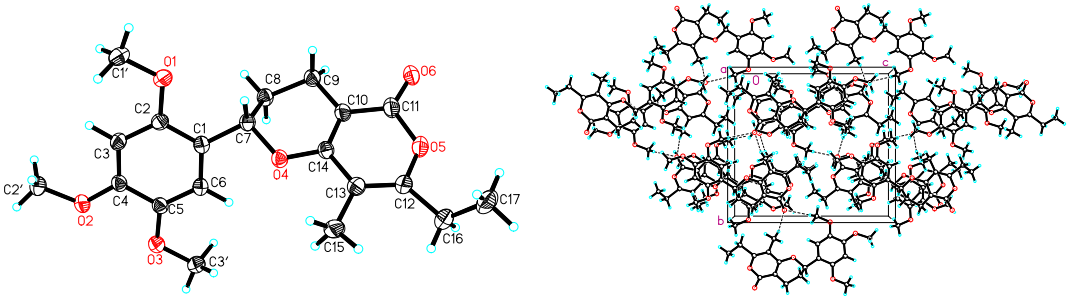

Figure S13. X-ray ORTEP drawing of **(-)-3** at the 50% probability levels.

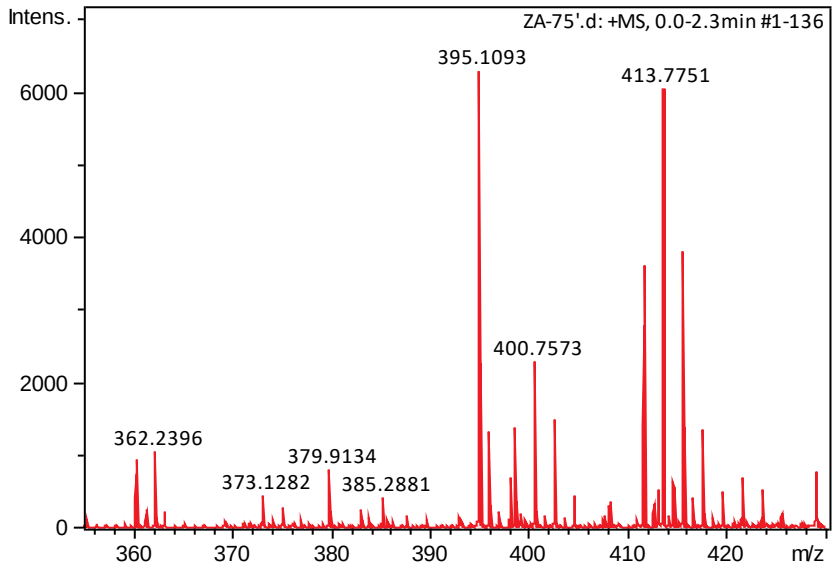

Figure S14. HRMS(ESI) spectrum of **1**

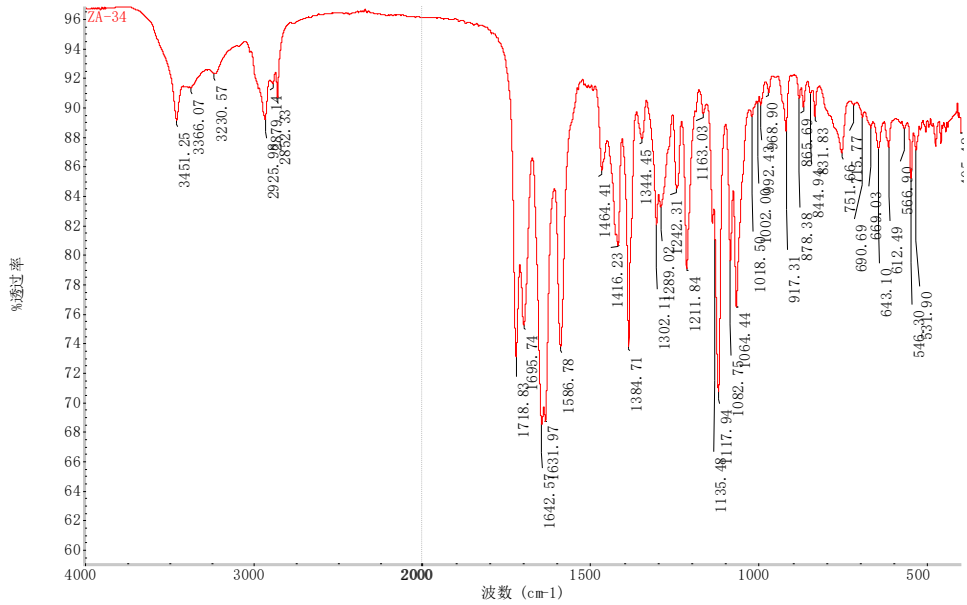

Figure S15. IR spectrum of **1**

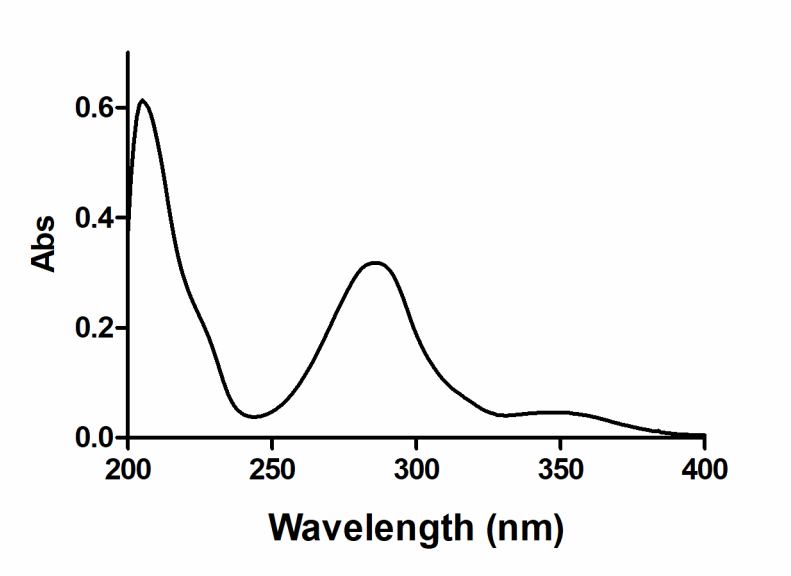

Figure S16. UV spectrum of **1**

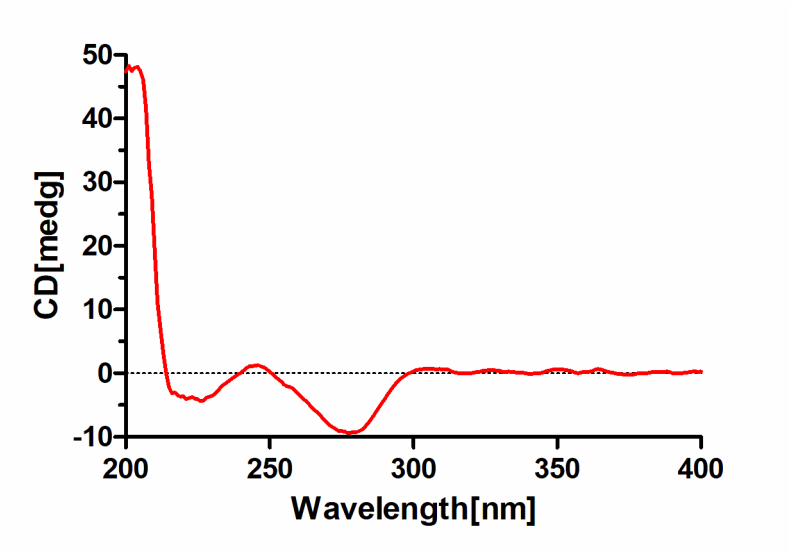

Figure S17. ECD spectrum of (+)-**1**

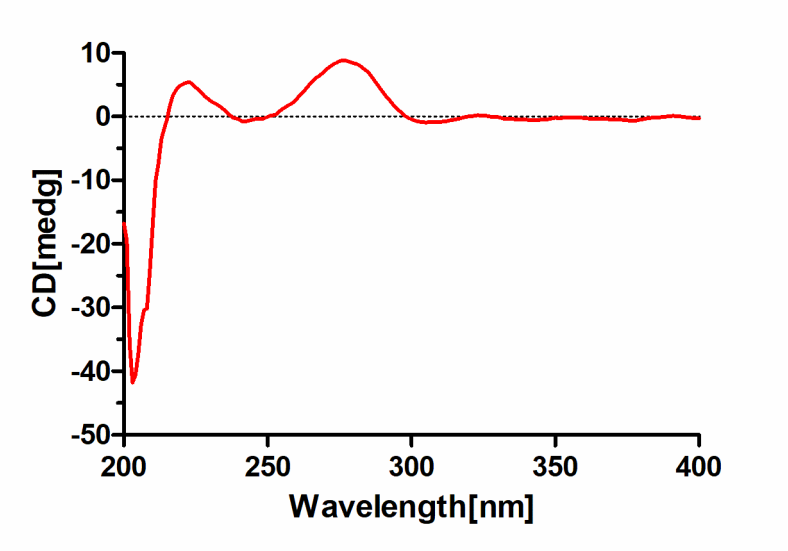

Figure S18. ECD spectrum of (-)-**1**

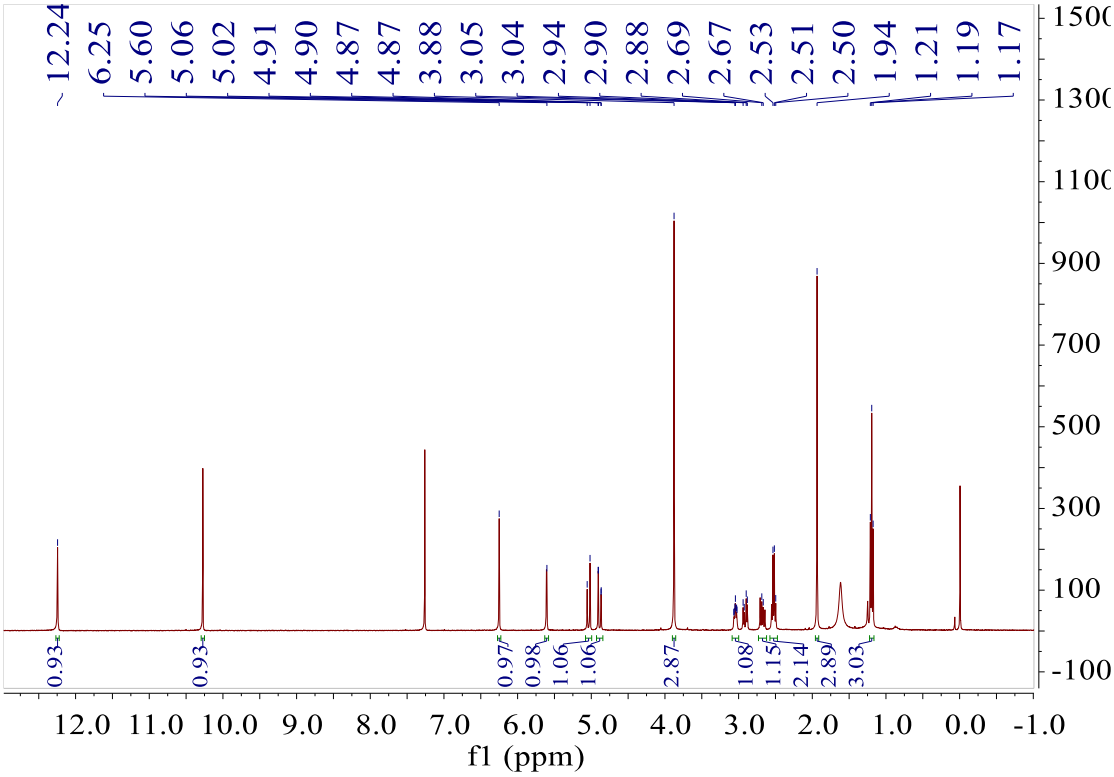

Figure S19. ^{1}H NMR spectrum (400 MHz, $CDCl_3$) of **1**

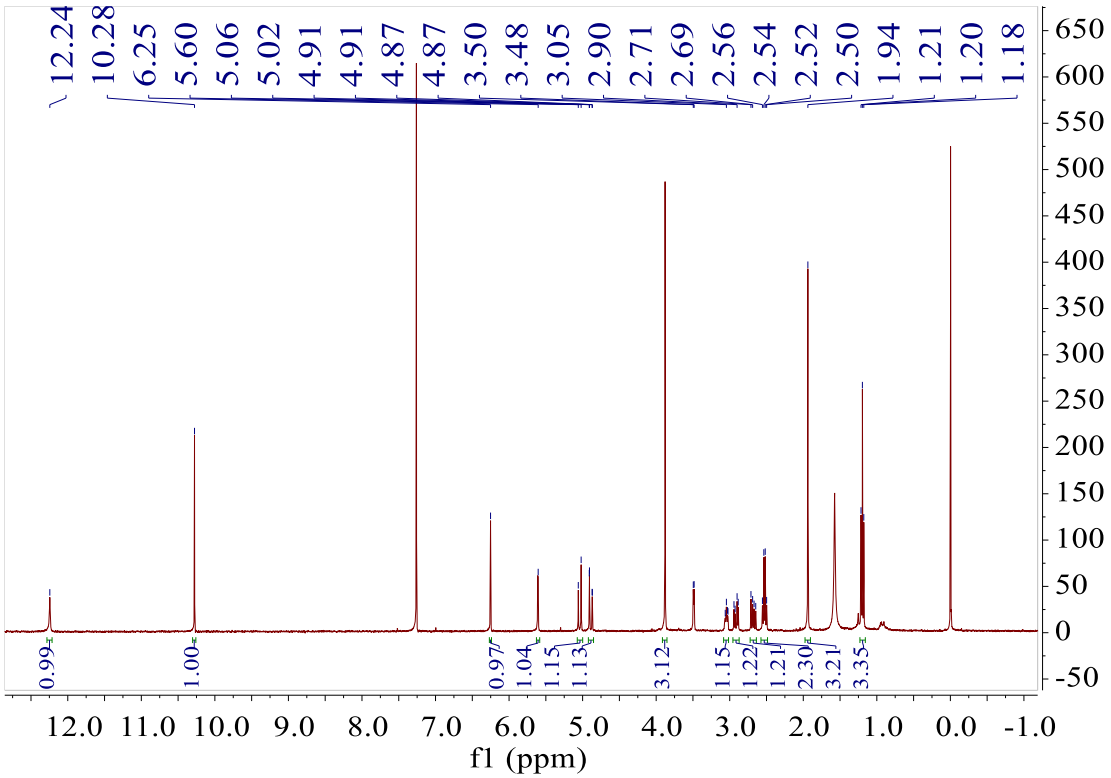

Figure S20. ^{1}H NMR spectrum (400 MHz, $CDCl_3$) of (+)-**1**

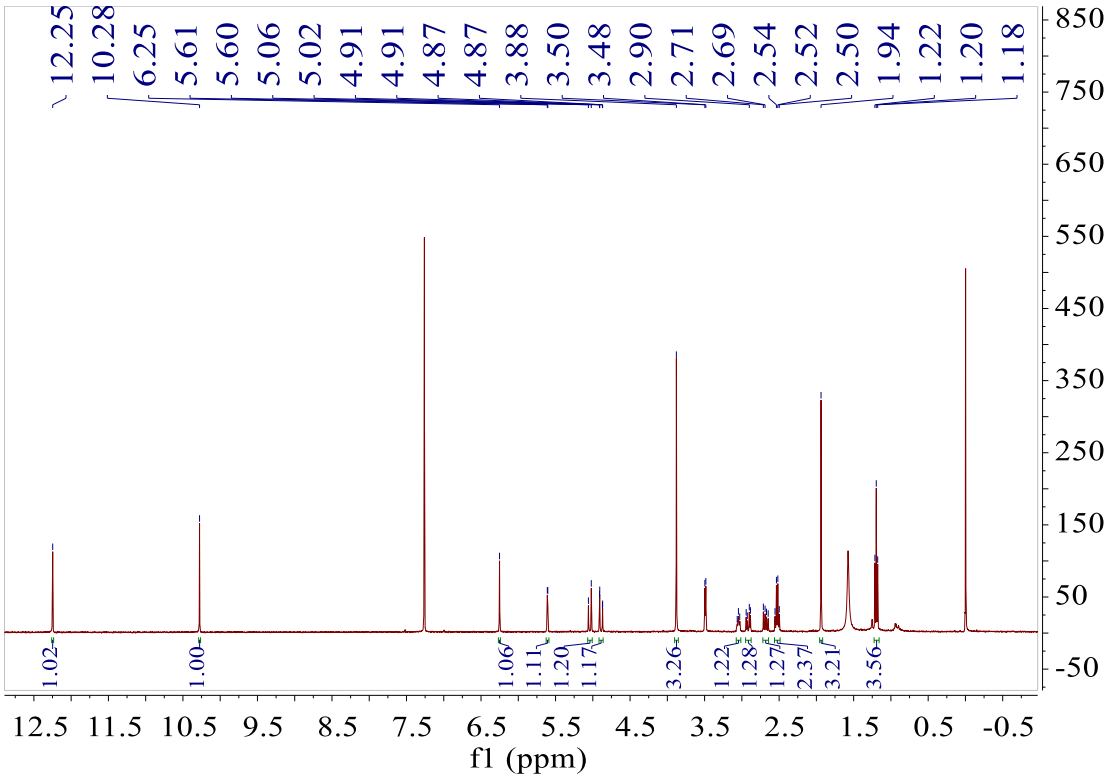

Figure S21. ^{1}H NMR spectrum (400 MHz, $CDCl_3$) of (-)-**1**

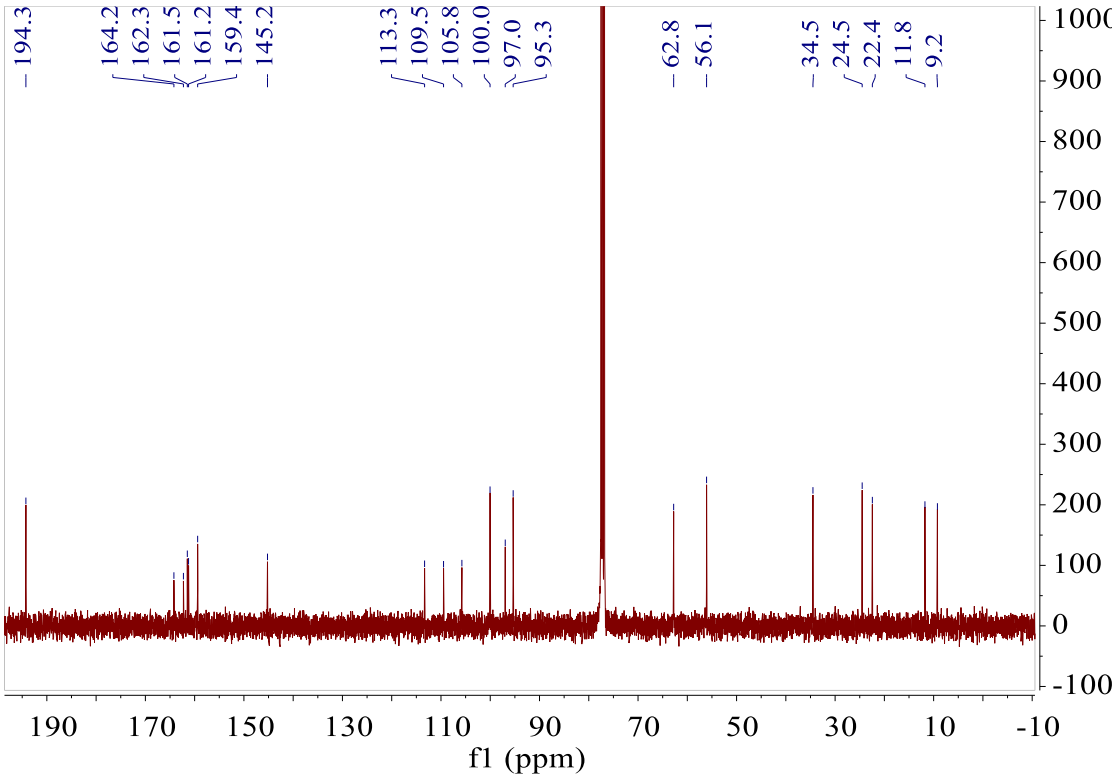

Figure S22. ^{13}C NMR spectrum (100 MHz, $CDCl_3$) of **1**

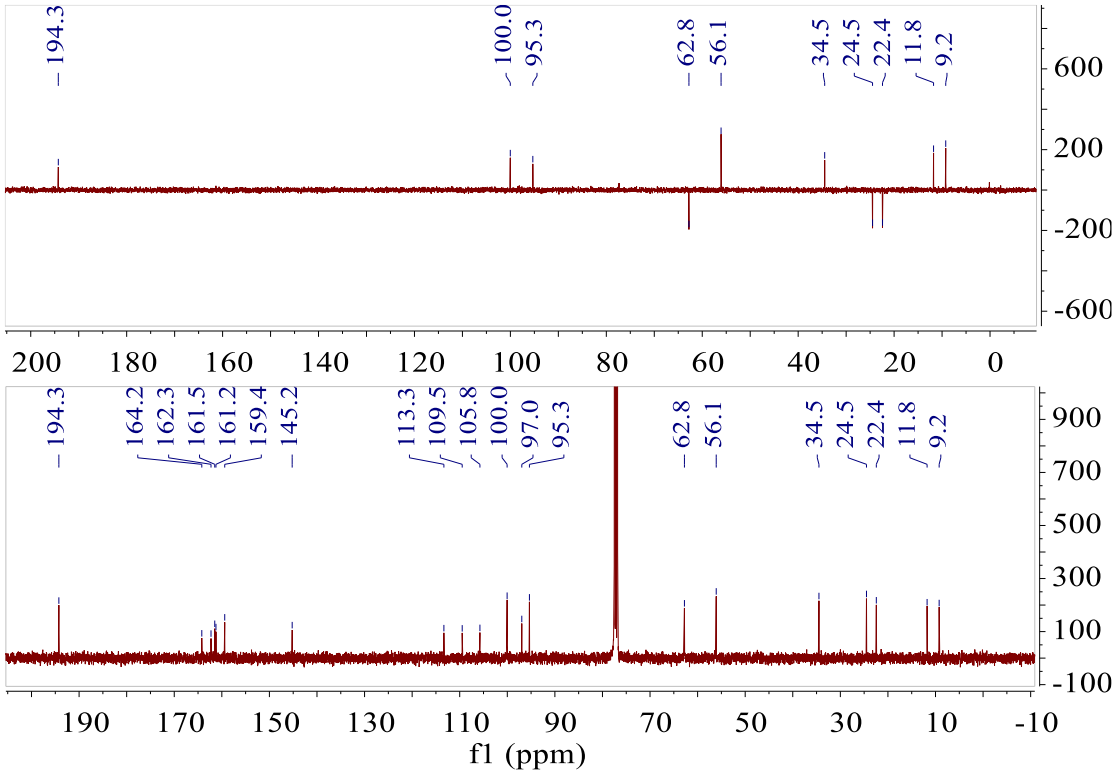

Figure S23. DEPT-135 spectrum (100 MHz, $CDCl_3$) of **1**

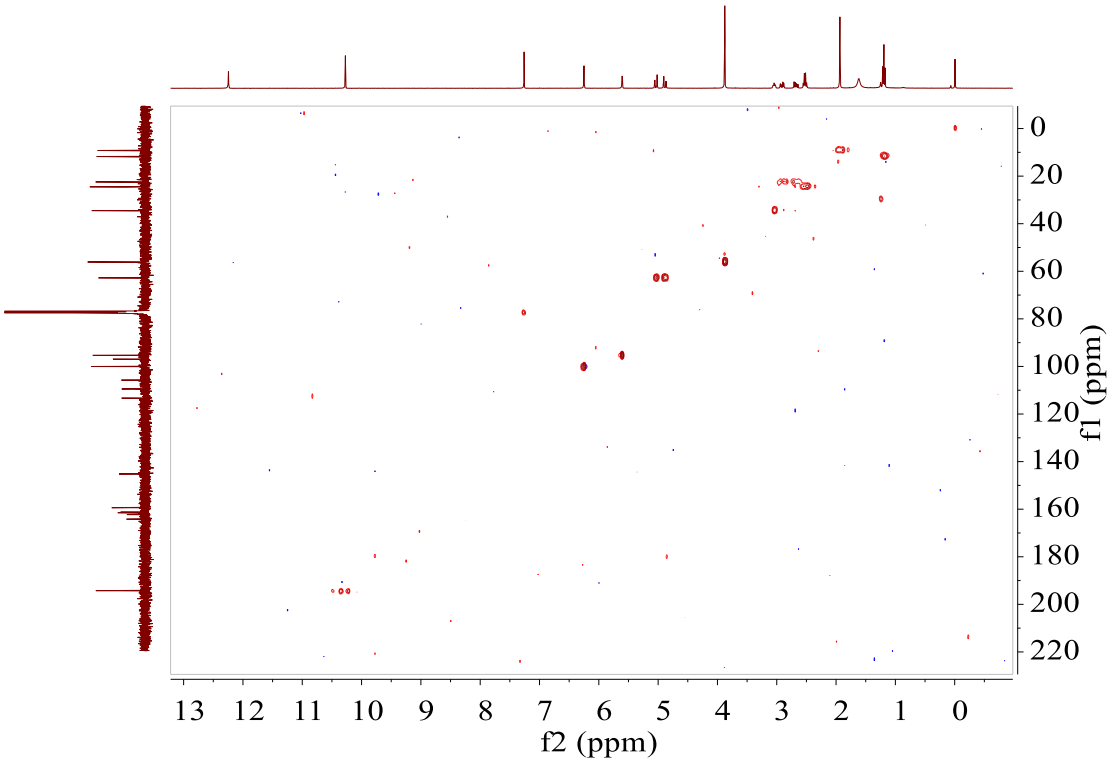

Figure S24. HSQC spectrum (400 MHz, $CDCl_3$) of **1**

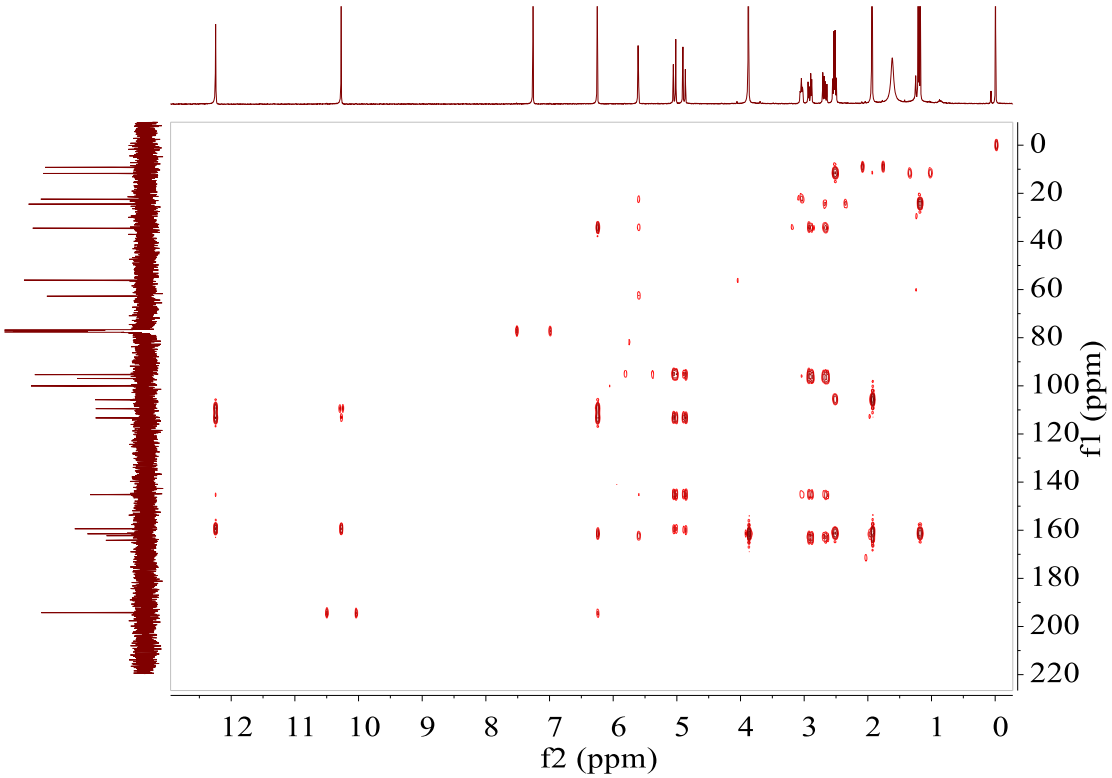

Figure S25. HMBC spectrum (400 MHz, $CDCl_3$) of **1**

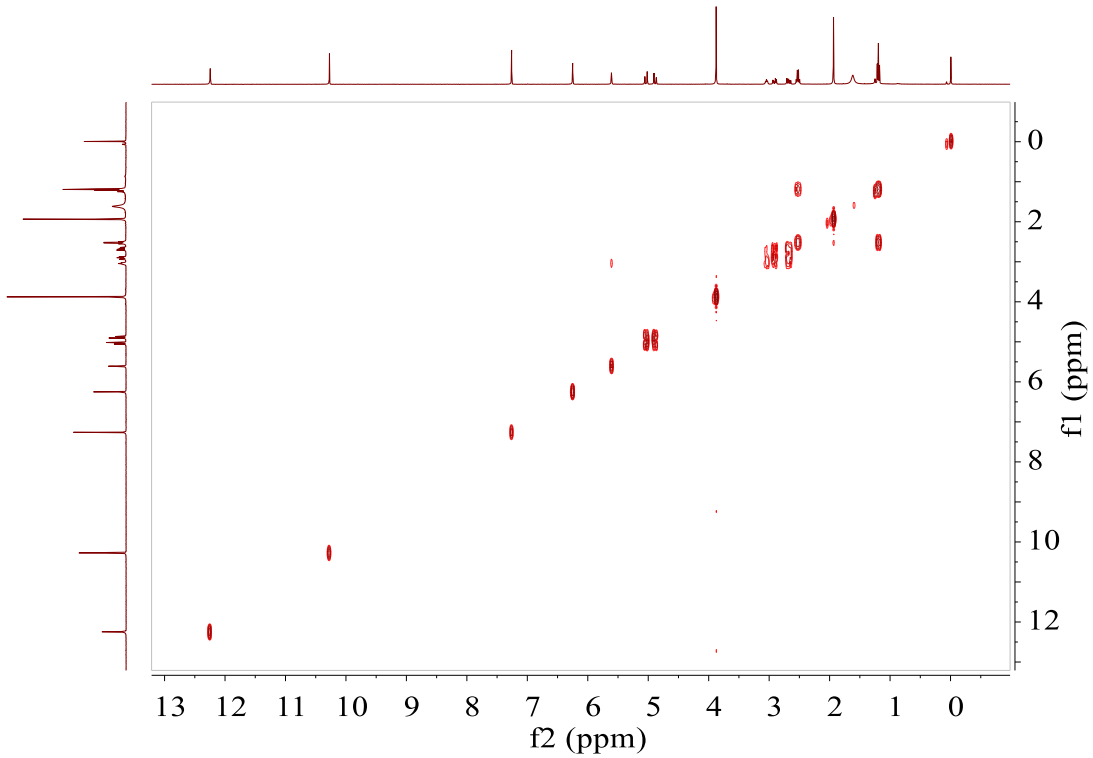

Figure S26. ^{1}H-^{1}H COSY spectrum (400 MHz, $CDCl_3$) of **1**

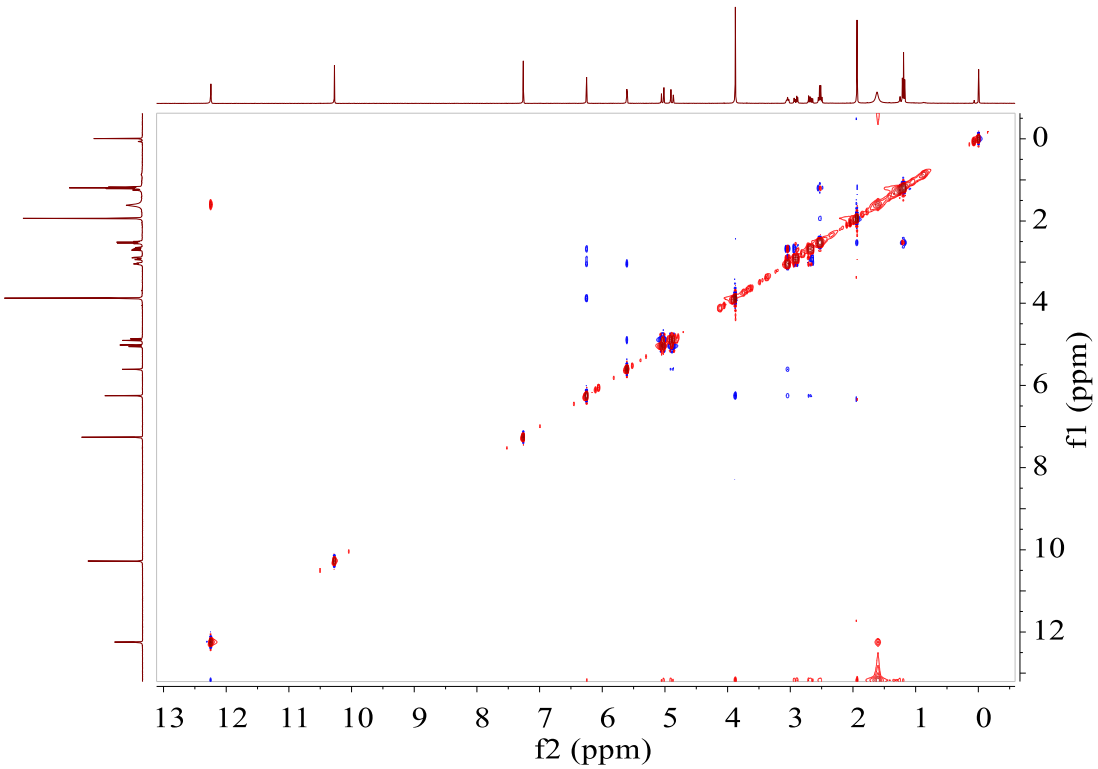

Figure S27. NOESY spectrum (400 MHz, $CDCl_3$) of **1**

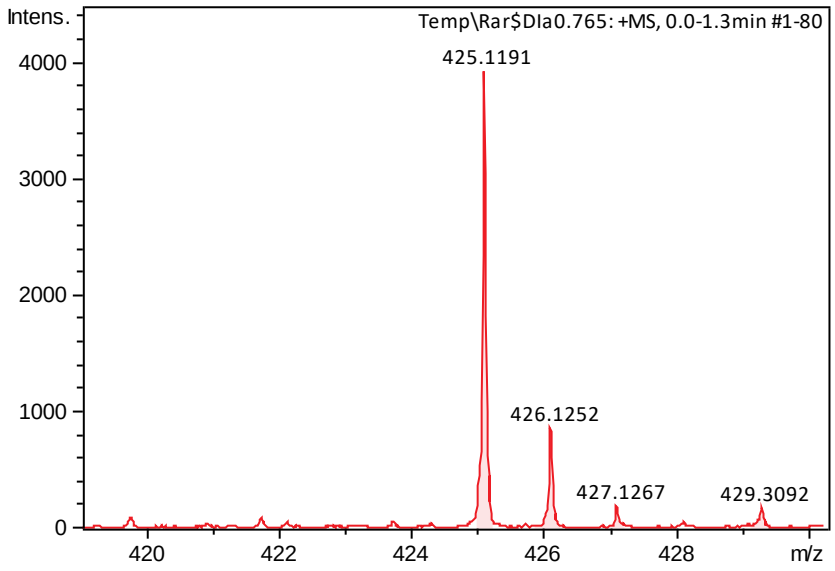

Figure S28. HRMS(ESI) spectrum of **2**

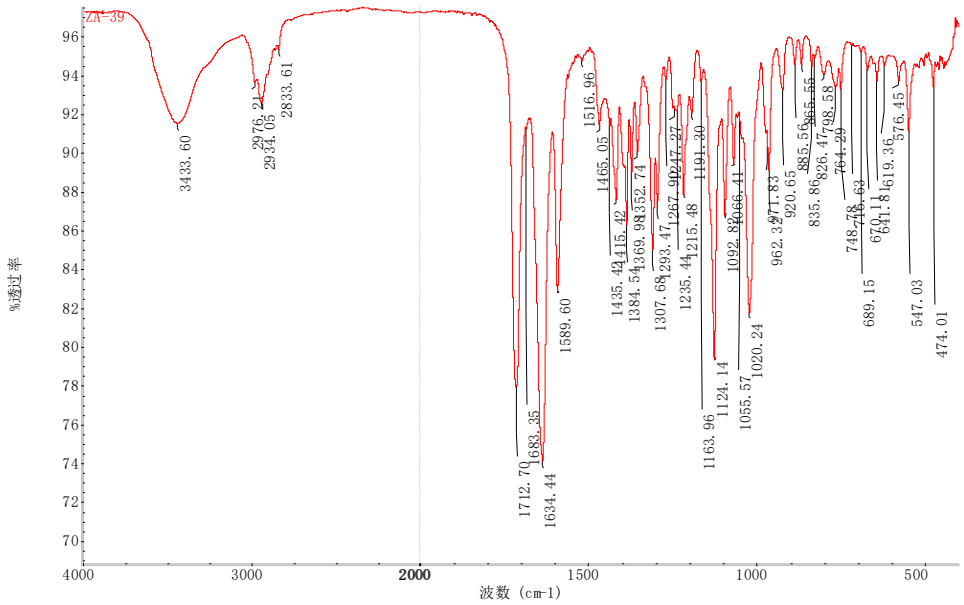

Figure S29. IR spectrum of **2**

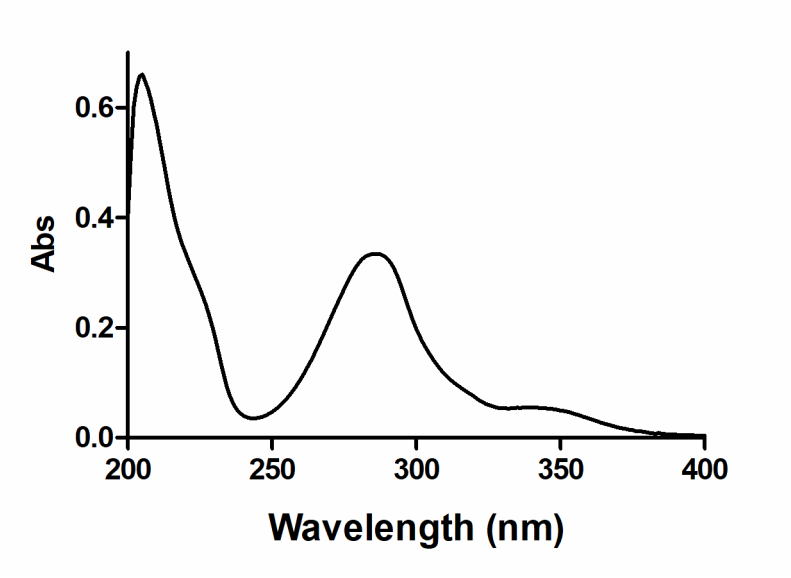

Figure S30. UV spectrum of **2**

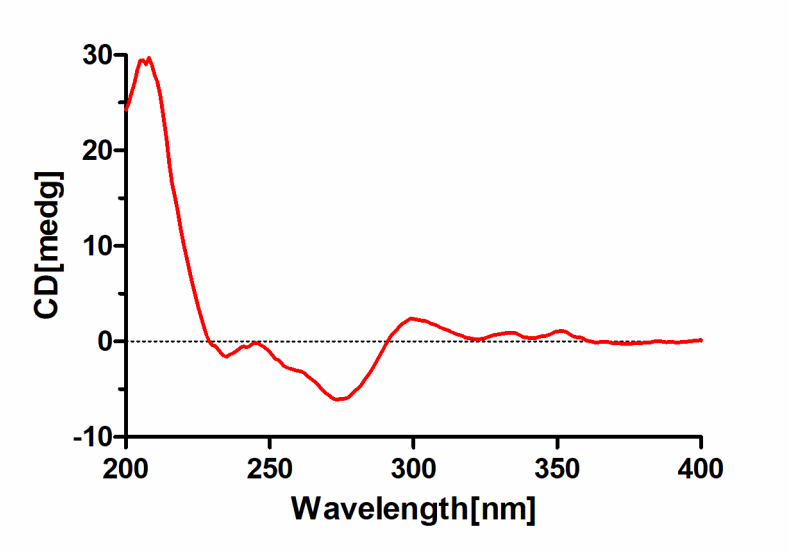

Figure S31. ECD spectrum of (+)-**2**

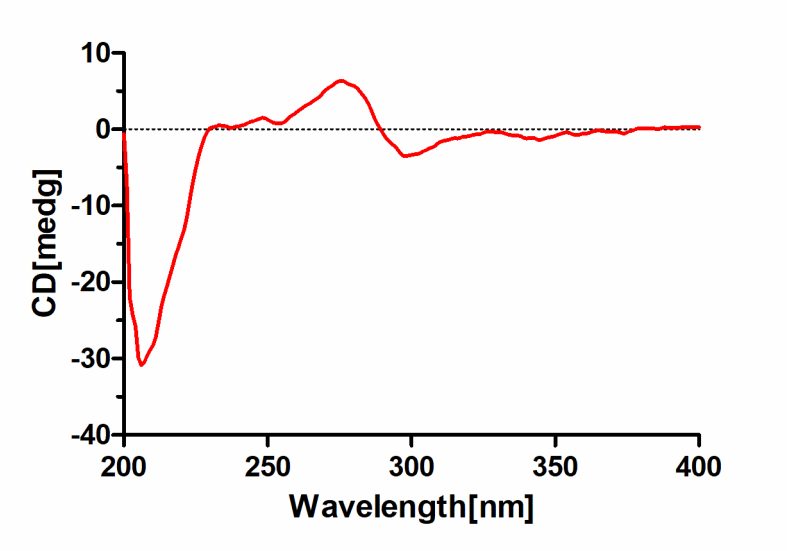

Figure S32. ECD spectrum of (-)-**2**

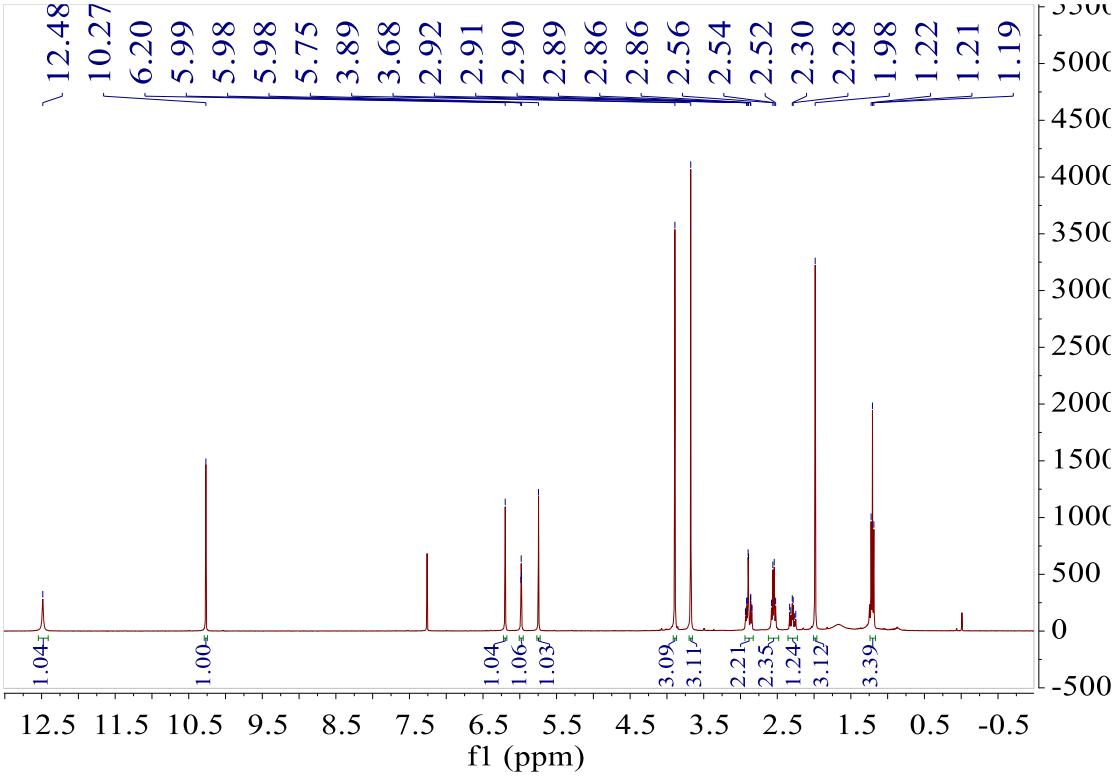

Figure S33. ^{1}H NMR spectrum (400 MHz, $CDCl_3$) of **2**

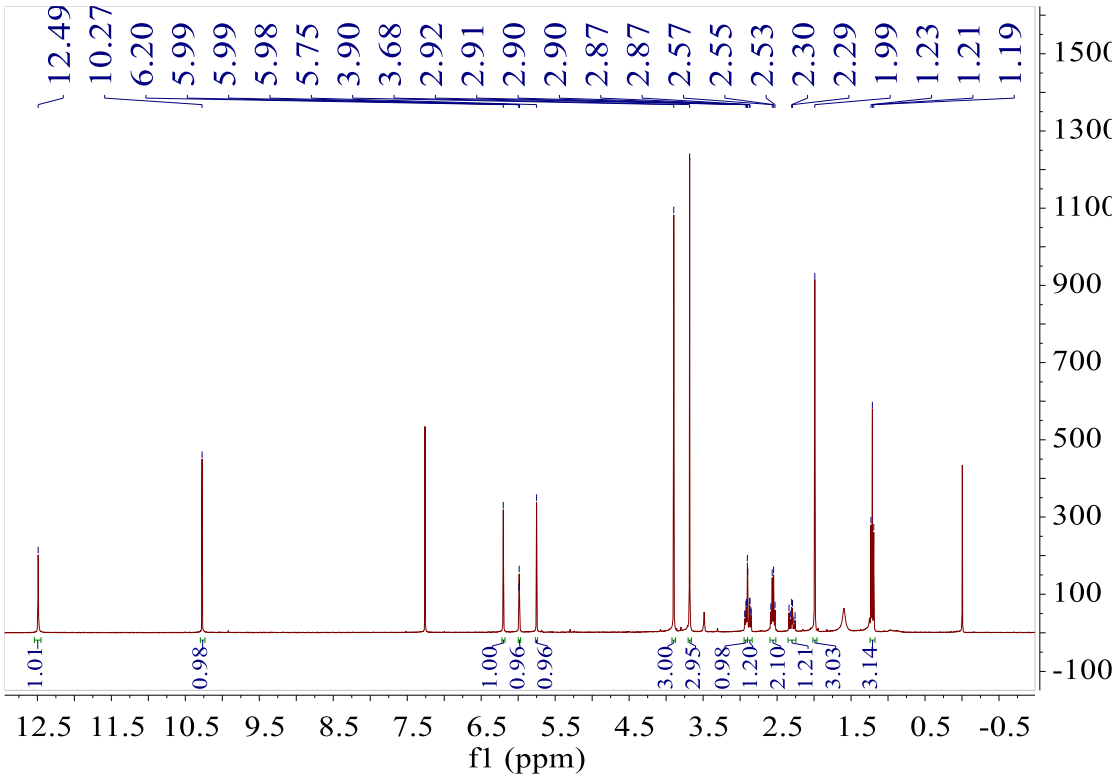

Figure S34. ^{1}H NMR spectrum (400 MHz, $CDCl_3$) of (+)-**2**

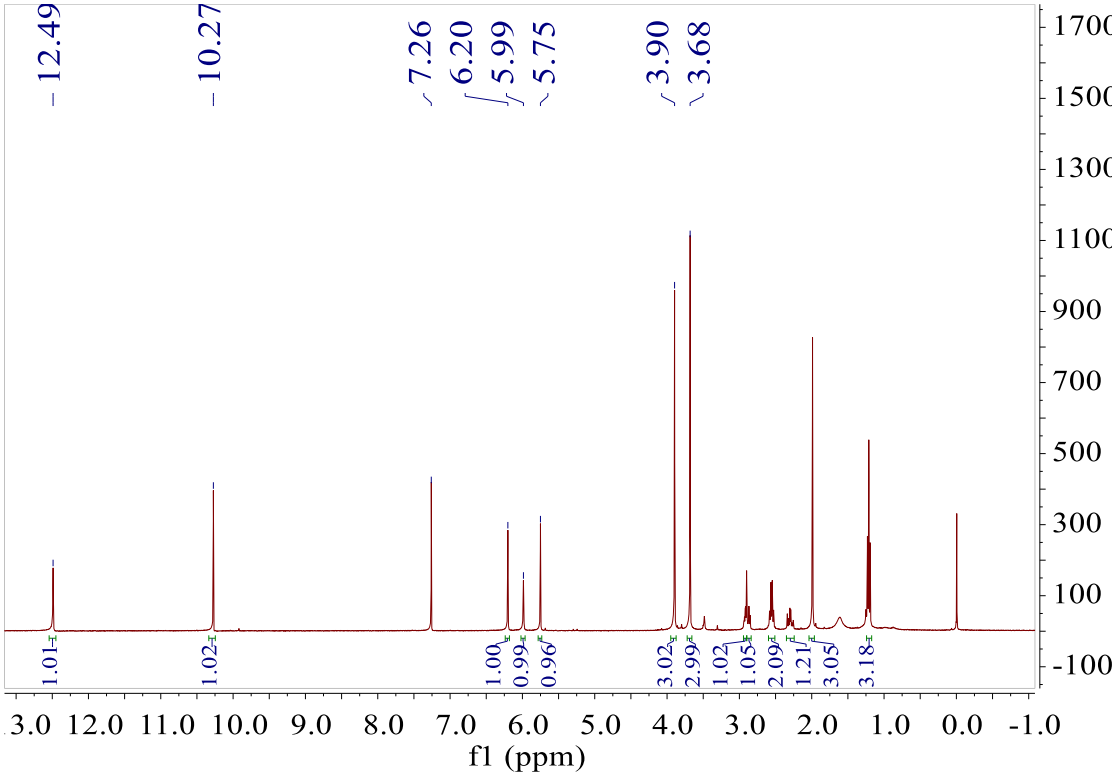

Figure S35. ^{1}H NMR spectrum (400 MHz, $CDCl_3$) of (-)-**2**

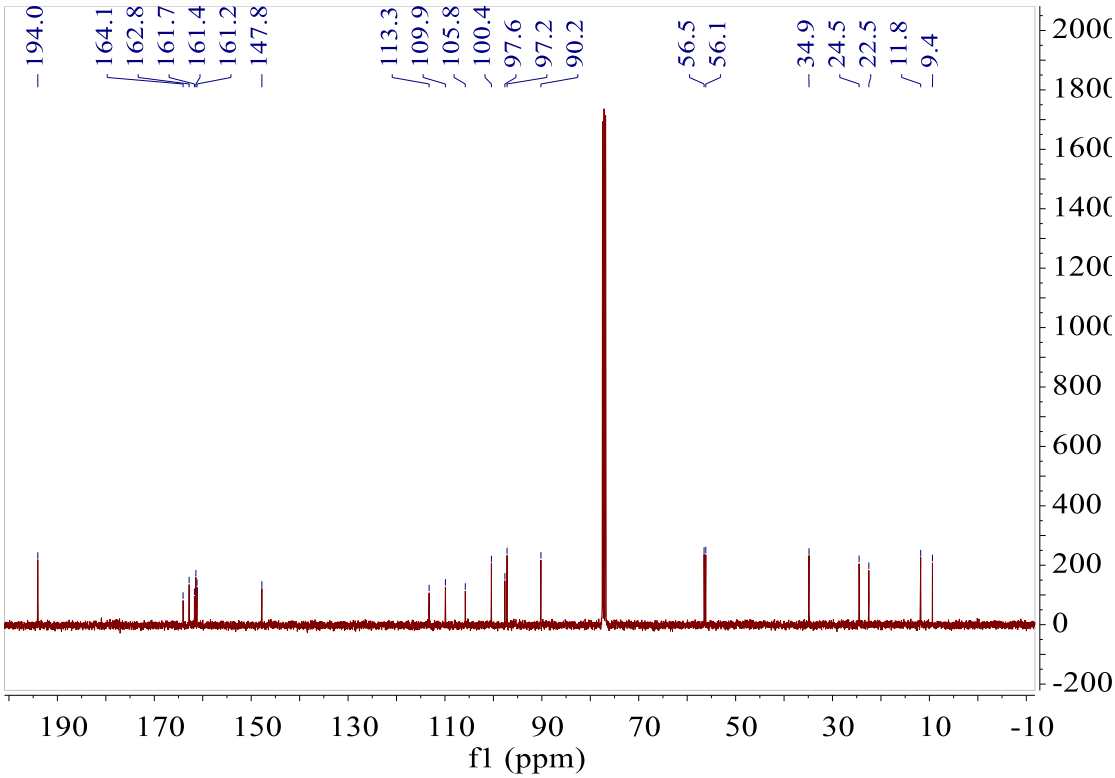

Figure S36. ^{13}C NMR spectrum (100 MHz, $CDCl_3$) of **2**

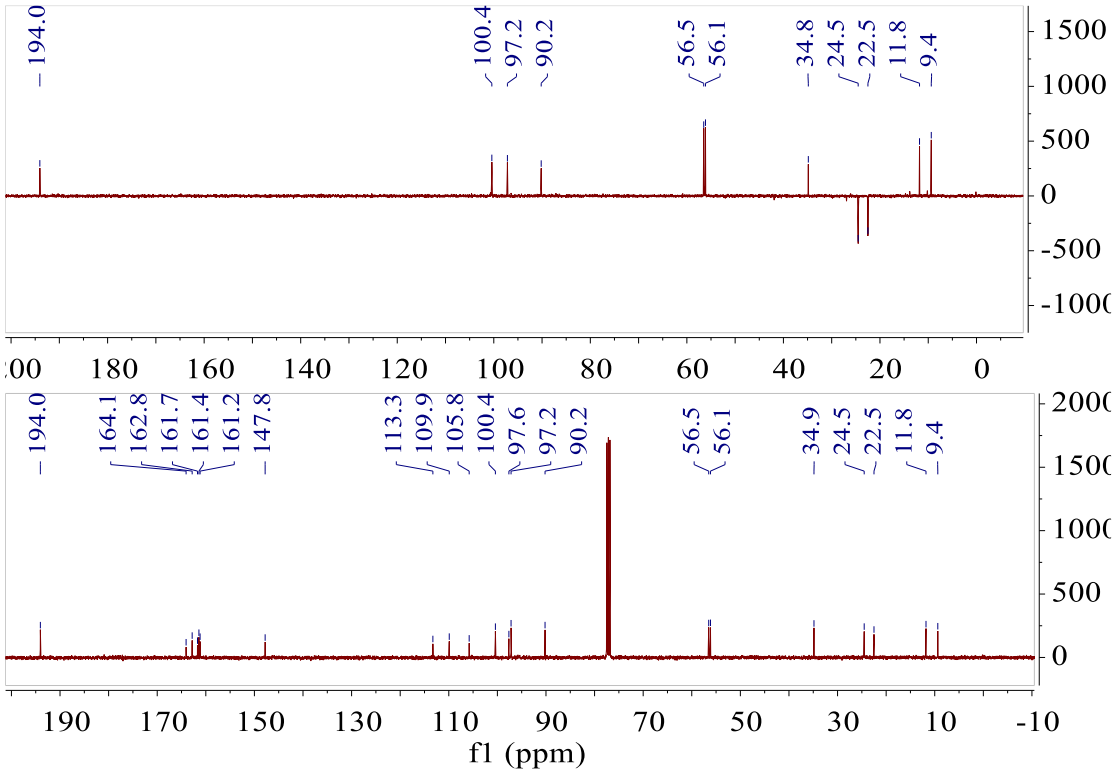

Figure S37. DEPT-135 spectrum (100 MHz, $CDCl_3$) of **2**

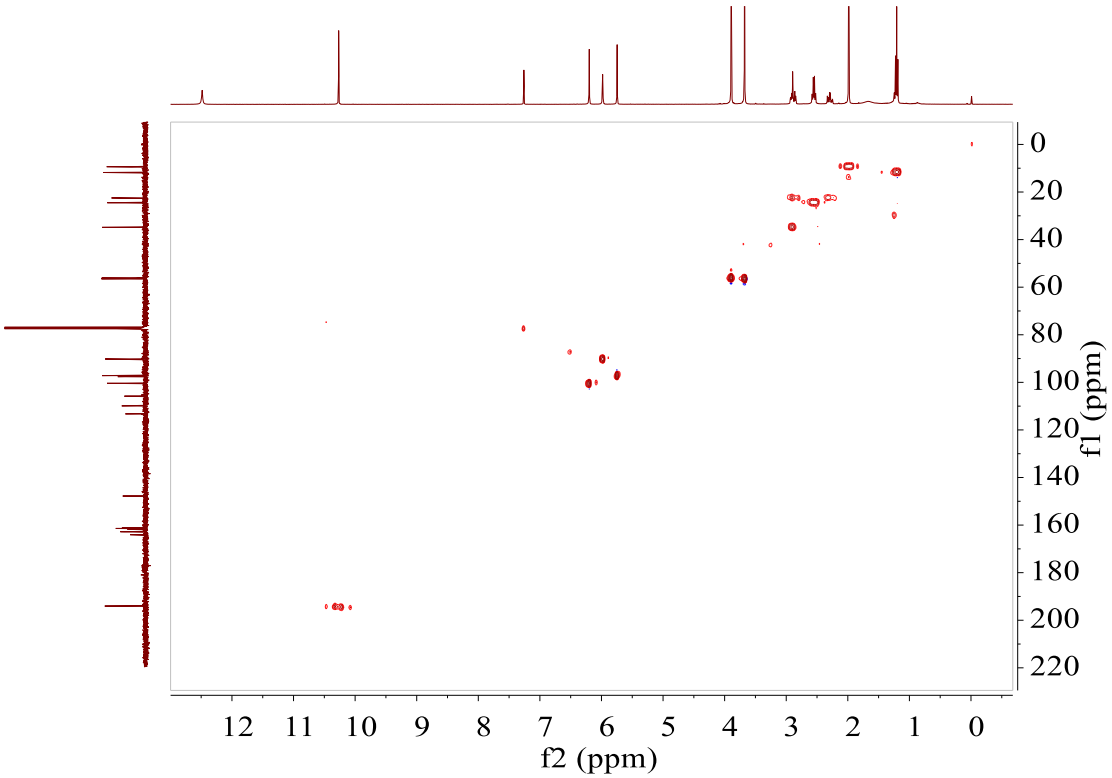

Figure S38. HSQC spectrum (400 MHz, $CDCl_3$) of **2**

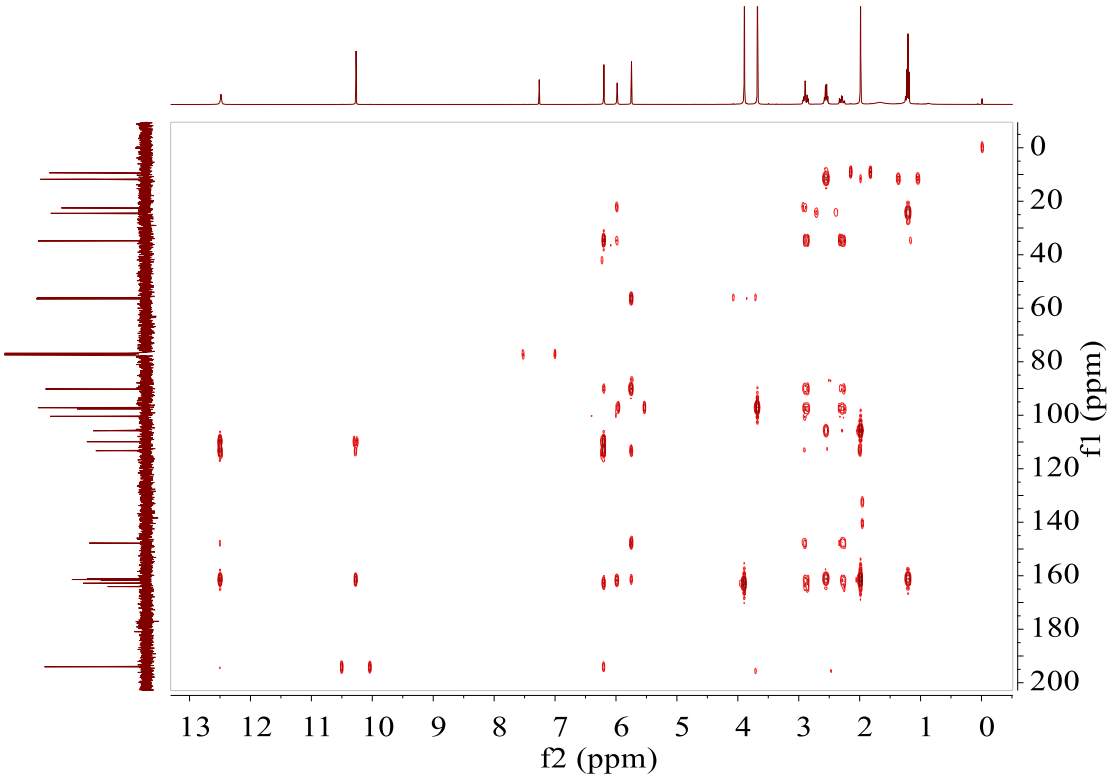

Figure S39. HMBC spectrum (400 MHz, $CDCl_3$) of **2**

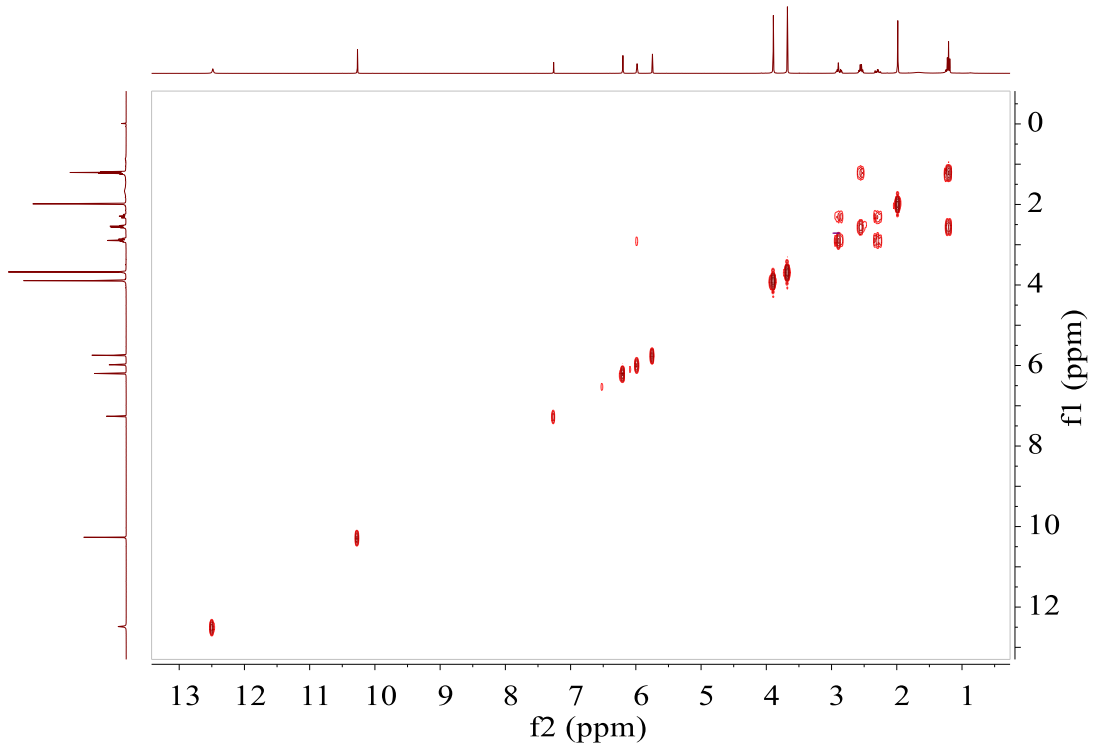

Figure S40. ^{1}H-^{1}H COSY spectrum (400 MHz, $CDCl_3$) of **2**

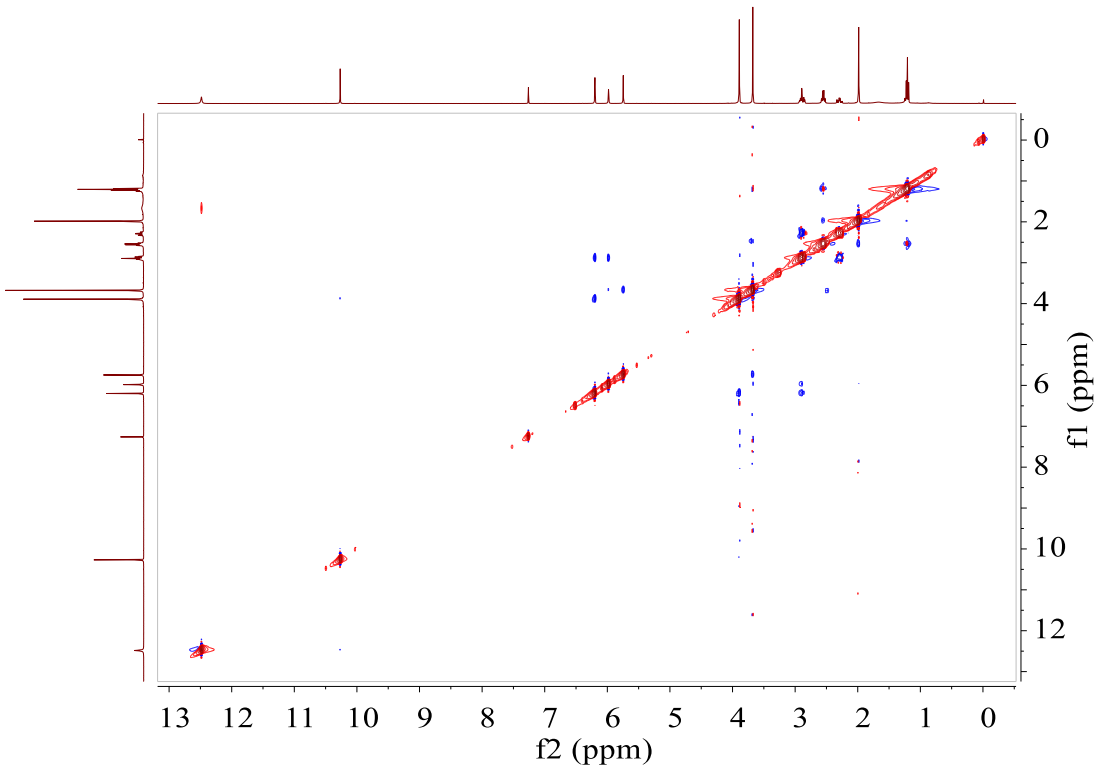

Figure S41. NOESY spectrum (400 MHz, $CDCl_3$) of **2**

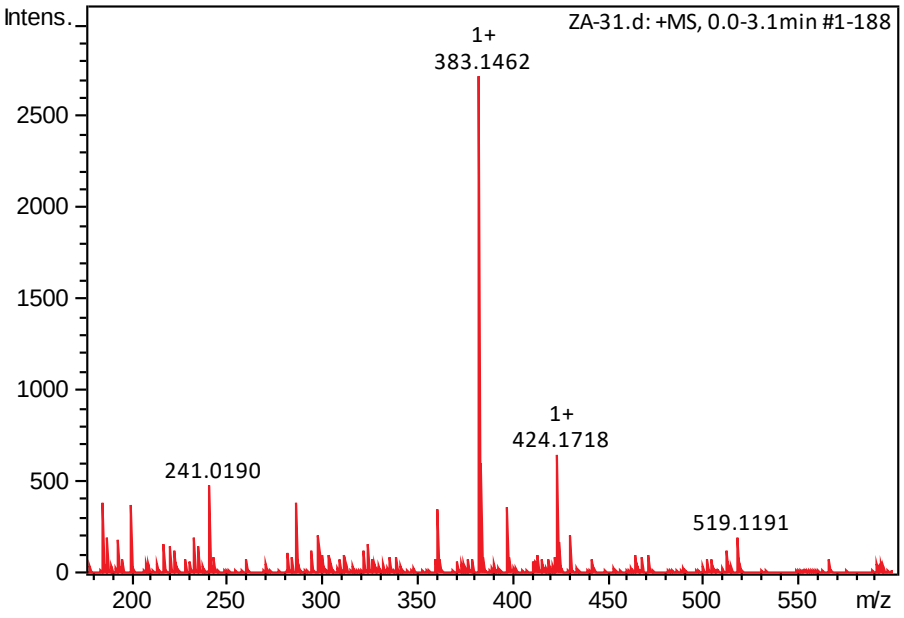

Figure S42. HRMS(ESI) spectrum of compound **3**

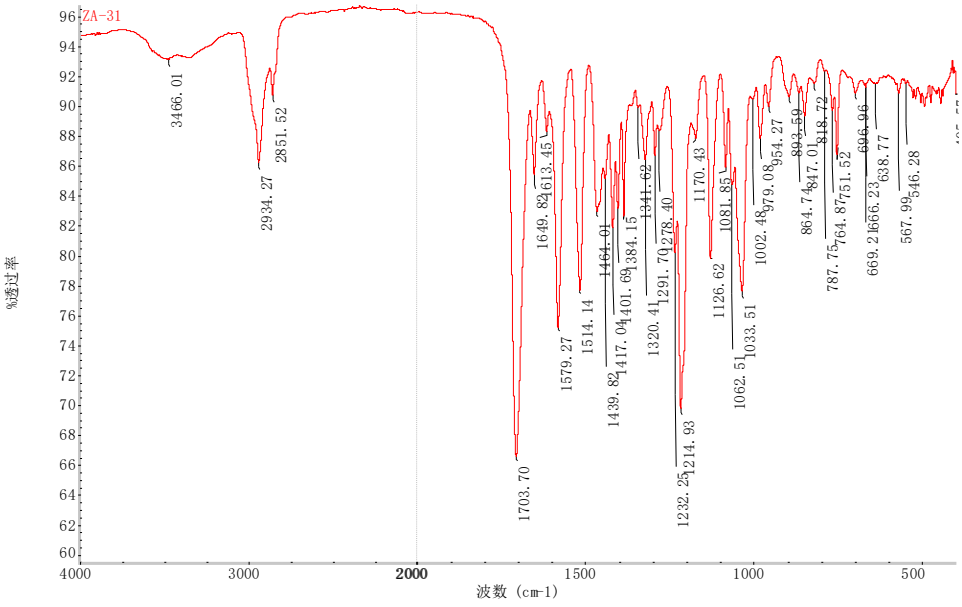

Figure S43. IR spectrum of **3**

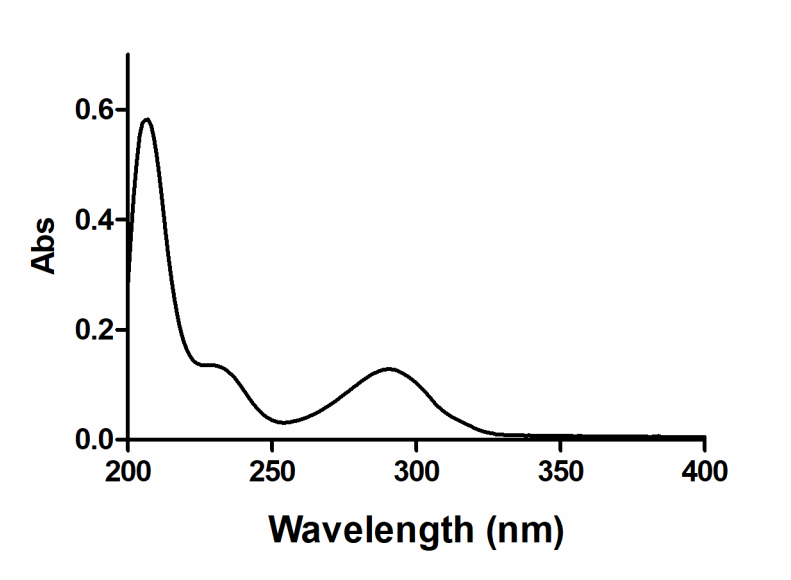

Figure S44. UV spectrum of **3**

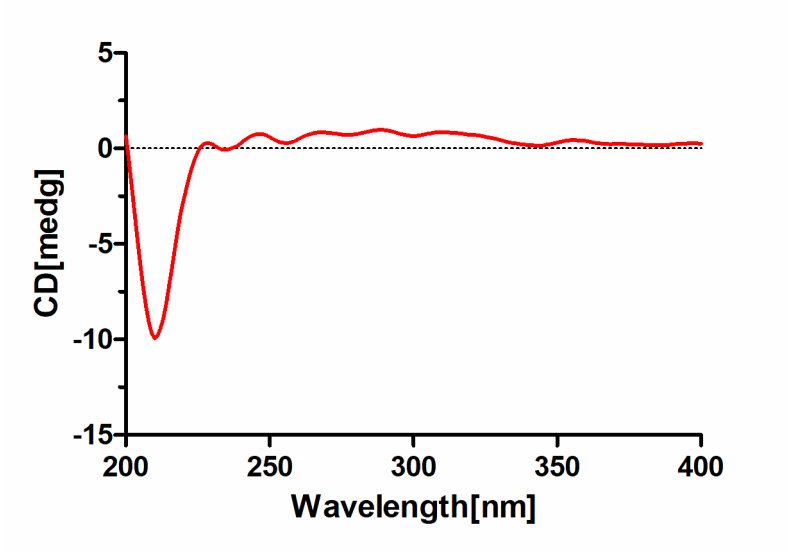

Figure S45. ECD spectrum of (+)-**3**

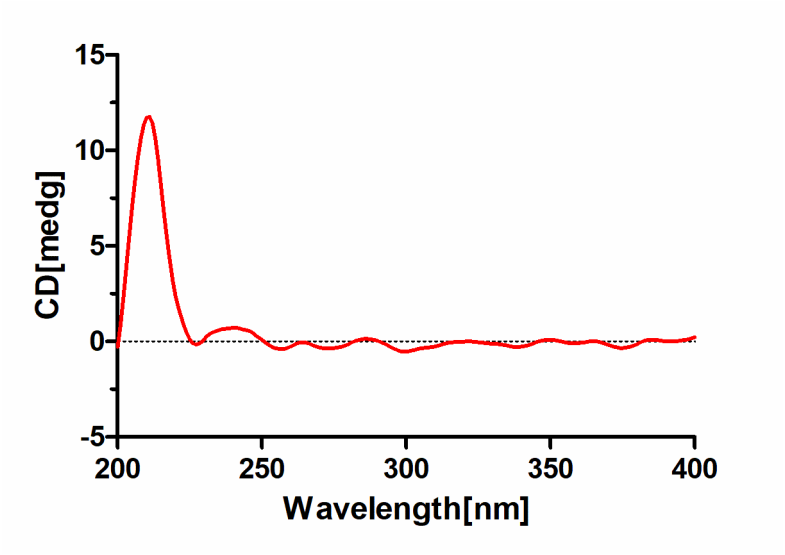

Figure S46. ECD spectrum of (-)-**3**

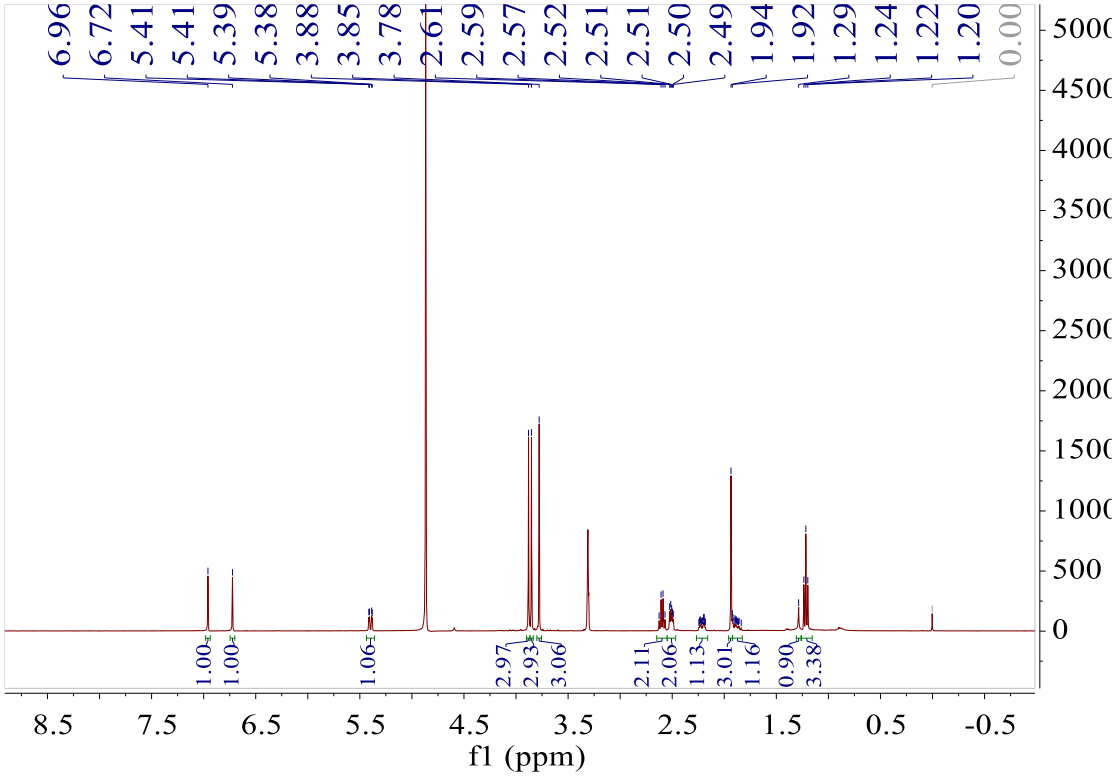

Figure S47. ^{1}H NMR spectrum (400 MHz, CD_3OD) of **3**

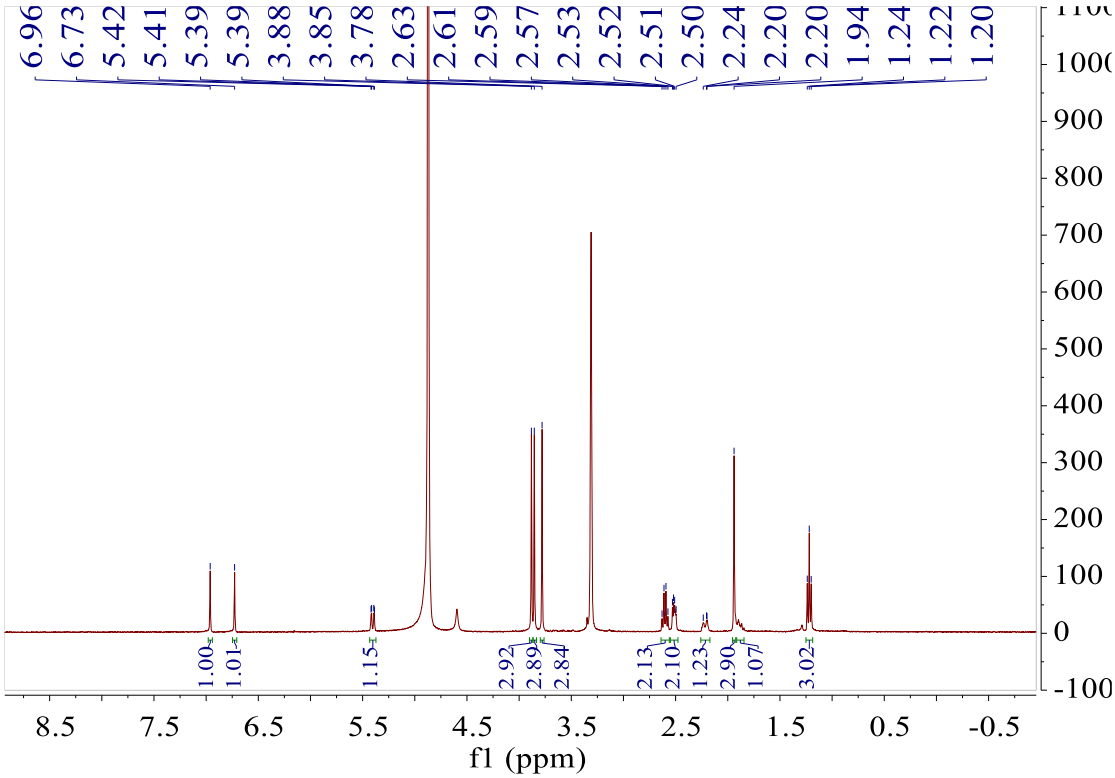

Figure S48. ^{1}H NMR spectrum (400 MHz, CD_3OD) of (+)-**3**

Figure S49. ^{1}H NMR spectrum

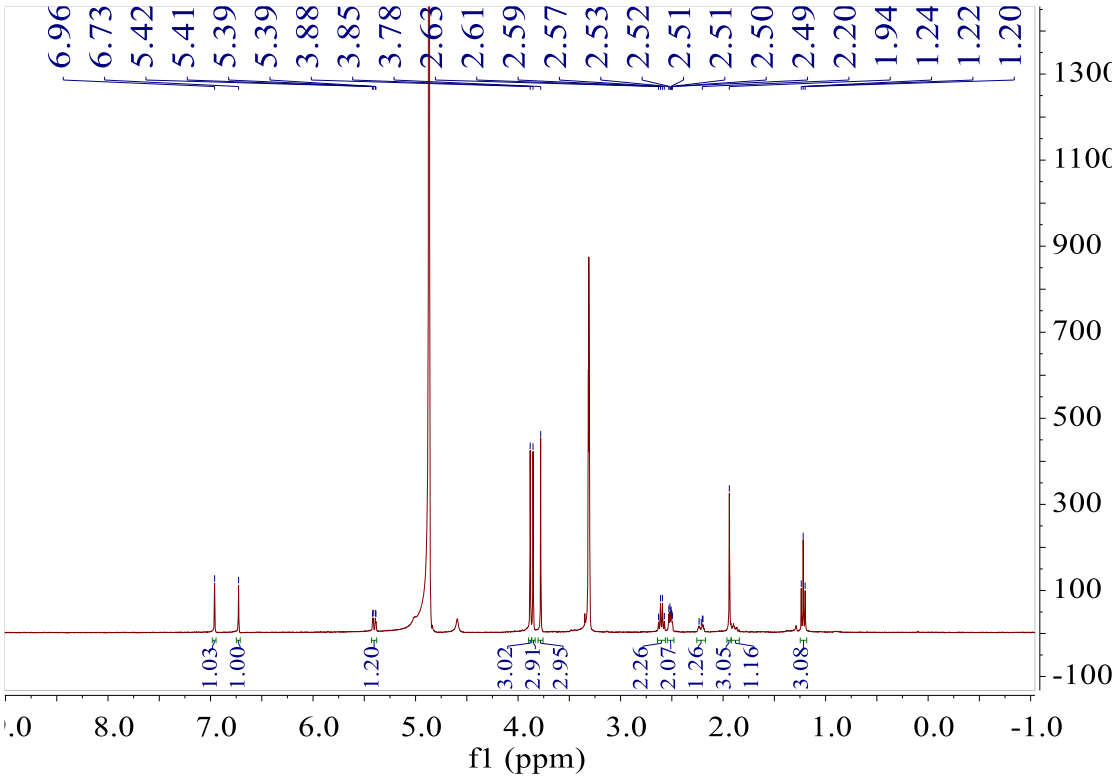

(400 MHz, CD_3OD) of (-)-**3**

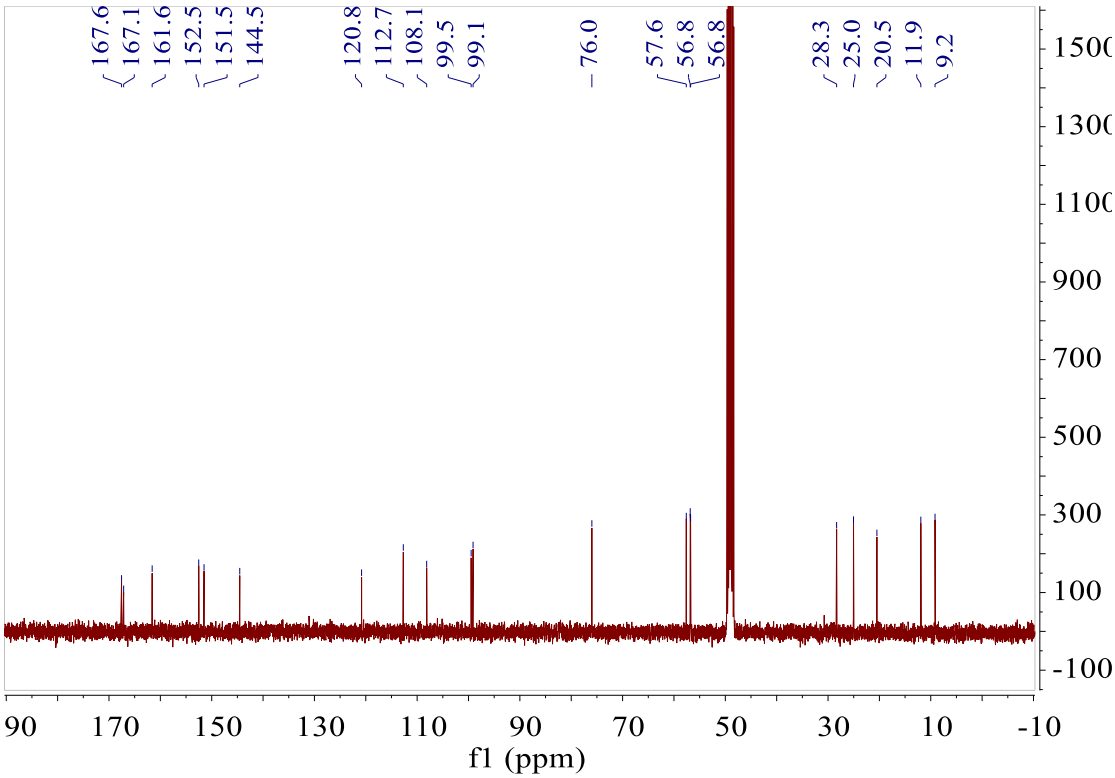

Figure S50. ^{13}C NMR spectrum (100 MHz, CD_3OD) of **3**

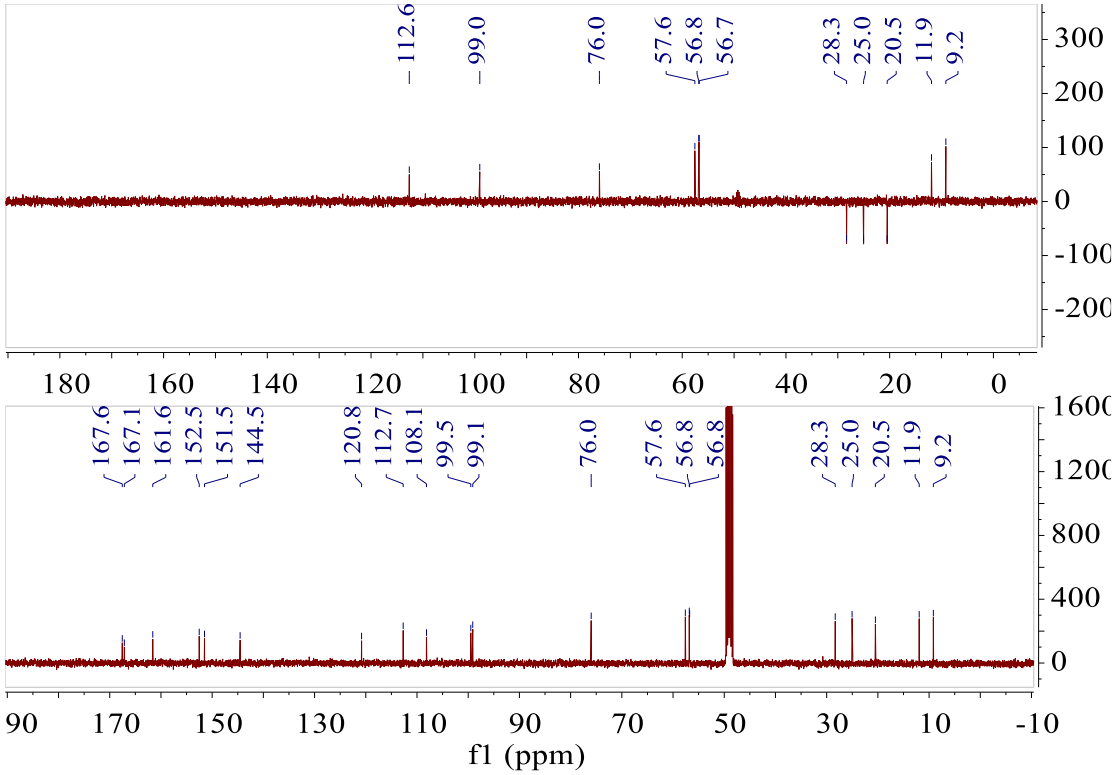

Figure S51. DEPT-135 spectrum (100 MHz, CD_3OD) of **3**

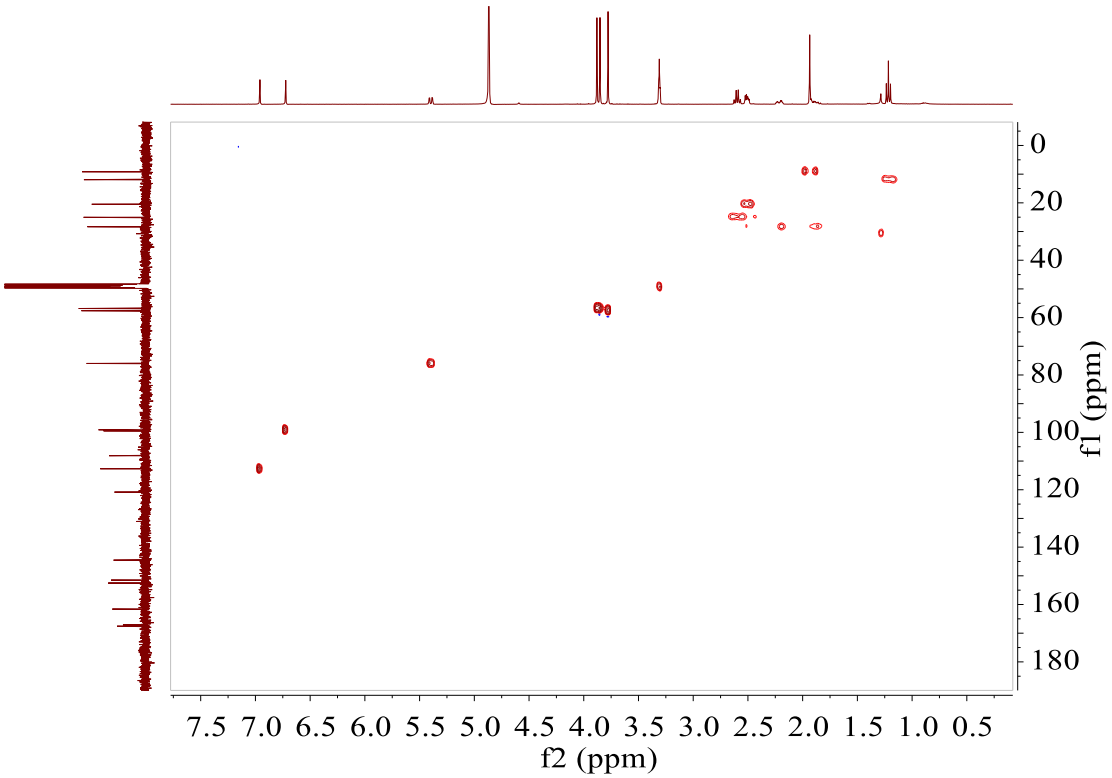

Figure S52. HSQC spectrum (400 MHz, CD_3OD) of **3**

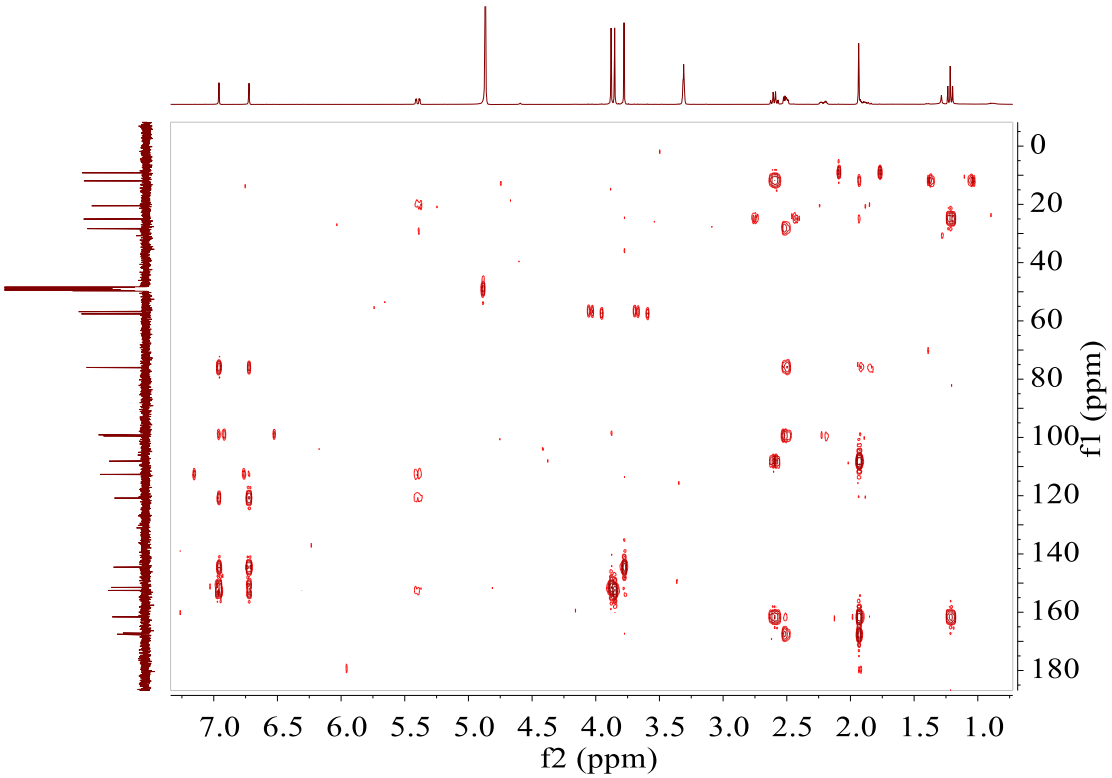

Figure S53. HMBC spectrum (400 MHz, CD_3OD) of **3**

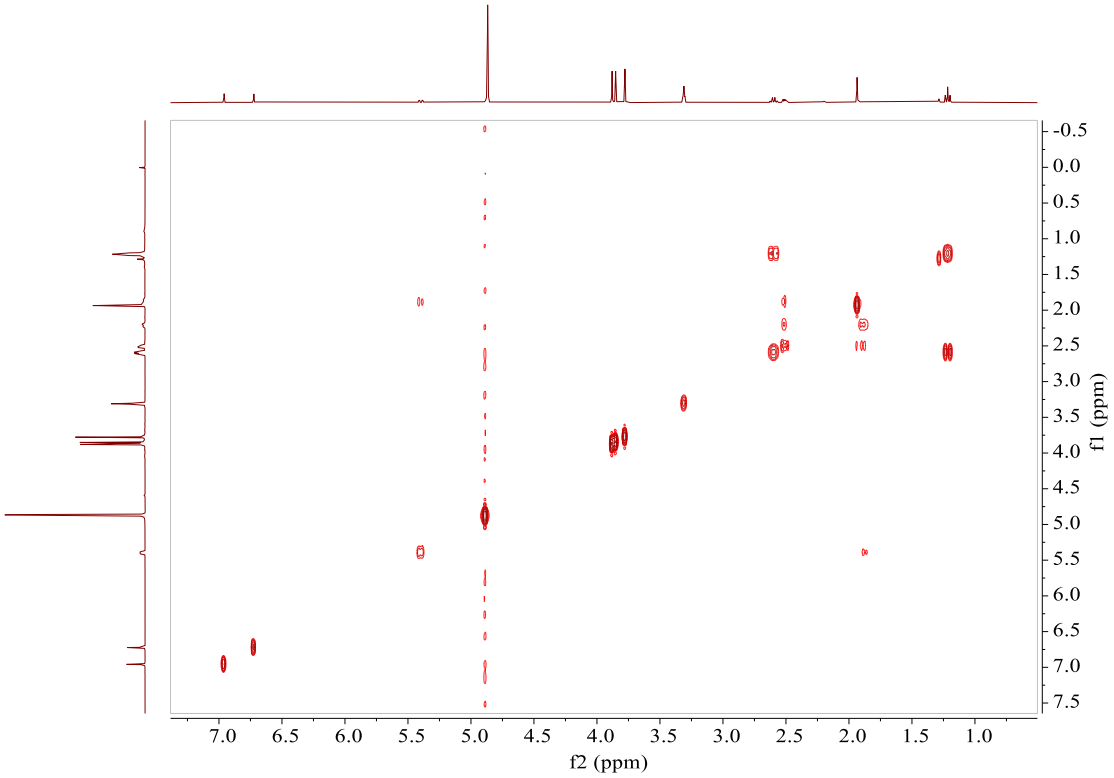

Figure S54. ^{1}H-^{1}H COSY spectrum (400 MHz, CD_3OD) of **3**

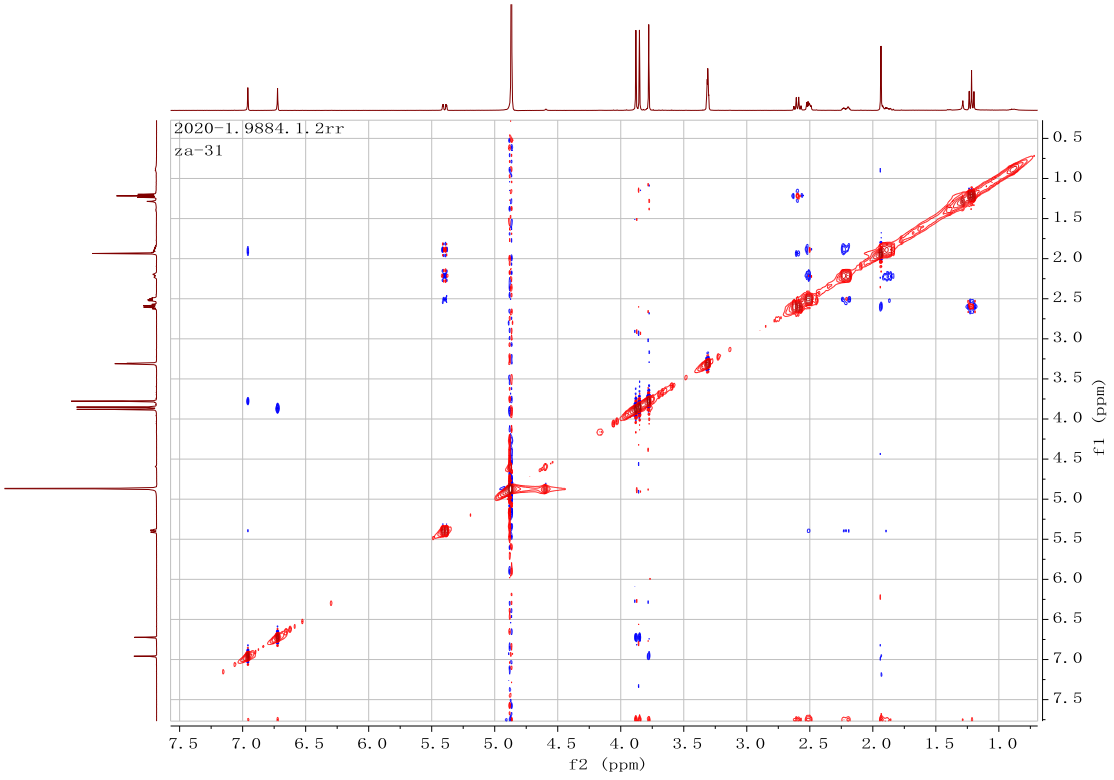

Figure S55. NOESY spectrum (400 MHz, CD_3OD) of **3**